Escola Tècnica Superior d'Enginyeria
Electrònica i Informàtica La Salle

Treball Final de Màster

Màster Universitari en Enginyeria de Telecomunicació

Ionospheric Polarization Diversity and Channel Study for Robust NVIS Remote Sensing Platforms

Alumne

Jordi Malé Carbonell

Professor Ponent

Joan Lluís Pijoan Vidal

ACTA DE L'EXAMEN
DEL TREBALL FI DE MÀSTER

Reunit el Tribunal qualificador en el dia de la data, l'alumne

D. Jordi Malé Carbonell

va exposar el seu Treball de Fi de Màster, el qual va tractar sobre el tema següent:

Ionospheric Polarization Diversity and Channel Study for Robust NVIS Remote Sensing Platforms

Acabada l'exposició i contestades per part de l'alumne les objeccions formulades pels Srs. membres del tribunal, aquest valorà l'esmentat Treball amb la qualificació de

Barcelona,

VOCAL DEL TRIBUNAL VOCAL DEL TRIBUNAL

PRESIDENT DEL TRIBUNAL

Ionospheric Polarization Diversity and Channel Study for Robust NVIS Remote Sensing Platforms

by

Jordi Malé Carbonell

Master's Degree in Telecommunication Engineering

Universitat Ramon Llull, La Salle BCN

September 2020

Abstract

Ionospheric Polarization Diversity and Channel Study for Robust NVIS Remote Sensing Platforms

by

Jordi Malé Carbonell

Master's Degree in Telecommunication Engineering

Universitat Ramon Llull, La Salle BCN

Professor Joan Lluís Pijoan Vidal, PhD

This project presents the complete study of a NVIS SIMO channel between the cities of Barcelona and Cambrils. This link benefits from the ionosphere's properties and uses polarization diversity. This document presents the comparation of different combining techniques, modulations, transmitting powers and channels.

The main objective of this work is to study and compare three different digital modulations, using them with a total of 5 different modulation orders and a complete power sweep. All the information and results are aimed in the improvement of the NVIS SIMO link implemented, increasing the robustness of the data transmission and the capacity if the system is upgraded to MIMO.

A part of the complete study of the link, a channel study is exhibited. Both the ordinary wave's channel and the extraordinary wave's channel are tested and compared with different parameters and the channels' yield.

In reference to the results obtained, the desired results have been achieved. The best setups for the link have been obtained with noteworthy results in terms of performance. These link configurations together with the channel study open new doors and horizons for the HF ionospheric communications, which appear to be a great solution for remote sensing networks.

Key Words

HF Communications; Ionosphere; NVIS; Digital Modulations; Channel Study; Polarization Diversity; Diversity Combining; SIMO; Remote Sensing; .

Contents

List of Figures

List of Tables

Acknowledgements

I would like to express my most sincere appreciation and gratitude to all the people that has been involved in the project. The great team behind this project, formed by Joaquim Porté, Josep Maria Masó, Tomás González, Dr Joan Lluís Pijoan and Dr David Badia have always given extraordinary support and advice on the subject. I would also like to thank my family, friends and Marta for their patience and confidence they have placed in me during these last years.

Chapter 1

Introduction

1.1 Project Objectives

Telecommunications are indispensable in the world we live in. We live in a society that connects people from very distant points of the globe instantly, allowing the exchange of information easily and swiftly. Looking at the evolution of these interactions, the world's communications have gone from communicating multiple millions of people to multiple billions of what we call "things". Actually, today's networks are completely focused on urban areas with a lot of devices (Lora-Wan, NB-IoT, Sigfox [1] [2]) and also many people (GSM, 3G, 4G).

These network present remarkable dimensions, but this does not prevent them to experience a lot of problems and challenges in remote areas. The main weakness for the deployment of these systems in isolated areas is often due to the rather complicated orography. Reaching the installation terrain and acquiring the necessary infrastructure is extremely complicated compared to urban areas. In such scenarios, the main solution is satellite communication, which results in a significant investment in complex infrastructure that makes the transceiver remarkably expensive to be integrated with a remote sensing platform [3].

A good solution to the obstacle presented is the technology studied in this work, which uses the ionosphere as a "mirror of the electromagnetic waves" to transport the information sent between from one point to another remote point. This alternative works in the HF band (High Frequency: 3 - 30MHz) and has several advantages in order to supply an isolated zone. Firstly, the overall cost of the infrastructure together with its maintenance and assembly, is much lower than the requirements of other technologies currently used. On the other hand, it depends only and exclusively on the Sun and how it ionises the atmosphere. This complex and almost random dependency favours us in the speed of installation and operation (with two antennas tuned to a specific frequency and using the ionosphere as a communication channel we would already have the telecommunications system assembled).

Isolated areas and post-catastrophe scenarios have an economically viable solution, which will be deeply studied in this project.

1.2 Document Structure

After the introduction in this chapter, Chapter 2 will define the NVIS communication technology, together with the main theoretical concepts on how the ionospheric channel behaves. It will also introduce the polarization diversity, focusing on the two characteristic waves of the ionosphere: the ordinary and the extraordinary waves. Diversity combining techniques and digital modulations will also be presented, as the experiment of the project will be based on those.

Chapter 3 will describe the setup of the environment of the whole system, featuring its antennas, phasing networks and its signal processing unit, the Redpitaya. This chapter will also explain all the measures done during the work, the scenario and the frames used.

Chapter 4 will analyse all the results obtained while doing the measures explained in Chapter 3. A comparison between the different diversity combining techniques is presented, together with a power study.

Chapter 5 will also analyse all the results obtained, but it will focus on the comparison of the two ionospheric channels: the ordinary and the extraordinary. The doppler shift, doppler spread and the availability of the channels will be studied.

To conclude, chapter 6 will give an overview to all the work done in the project, and will end with the future research to be done based on the results obtained in this document.

Chapter 2

Theoretical Concepts

2.1 NVIS Communications

The ionosphere behaves like a mirror that enables communication in a large area when working inside a determinate range of frequencies. This mirror can be used in different ways depending on the incidence of the radio wave emitted: Firstly, horizontal incidence creates long-distance links that can cover the whole globe with few radio hops. On the other hand, if the radio wave is propagated vertically (or with a near vertical propagation), the ionosphere creates a wide area of coverage. This work is focused on the study of the Near Vertical Incidence Skywave (NVIS), a technique based on a vertical propagation of radio waves that reflect with the ionosphere.

As introduced in the previous chapter, this technology is pretty unique, as it enables communication between points without line of sight without the need of any complex infrastructure or network (NVIS is a fast and cheap technique). Figure 2.1 shows how a NVIS system overcomes the obstacles that may interfere the line of sight with the reflection in the atmosphere, resulting in a huge circular coverage.

NVIS communications rely completely in the reflection produced in the ionosphere. This reflection is entirely dependent on the frequency band and the angle of incidence of the radio wave.

- **Frequency Band:** Different frequencies imply different behaviours when talking about ionospheric communications. For NVIS systems, the band that must be used is HF (High Frequency, 3 - 30MHz). The selection of the frequency is unique for each experiment, and it has to be based on parameters such as the geographical position of the scenario and its radio-electric conditions. Typical frequencies are between 3 and 10 MHz [4]. The use of higher frequencies will eventually begin to worsen the performance of the ionospheric link, as the reflection will begin to be non-existent.

- **Angle of Incidence:** Near Vertical Incidence Skywave is based mainly on the direction of the radio wave. The angle of this wave must be elevated, tending to a perfectly right angle for the ionospheric link to work as desired, creating a large coverage area. Angles chosen are between 70^{o} and 90^{o} (90^{o} is known as VIS, Vertical Incidence Skywave), and create an area of approximately 250km radius of coverage without need of line of sight. Figure 2.1 gives a graphical idea on how the overall NVIS system functions, understanding the principle of the NVIS technologies. The figure also shows that no satellite or repeater is needed to make a communication between two distant points, confirming that NVIS is a system with simple infrastructure, easy to deploy and with a lower cost than other similar systems, such as 3G or 4G despite having lower bitrates and bigger antennas.

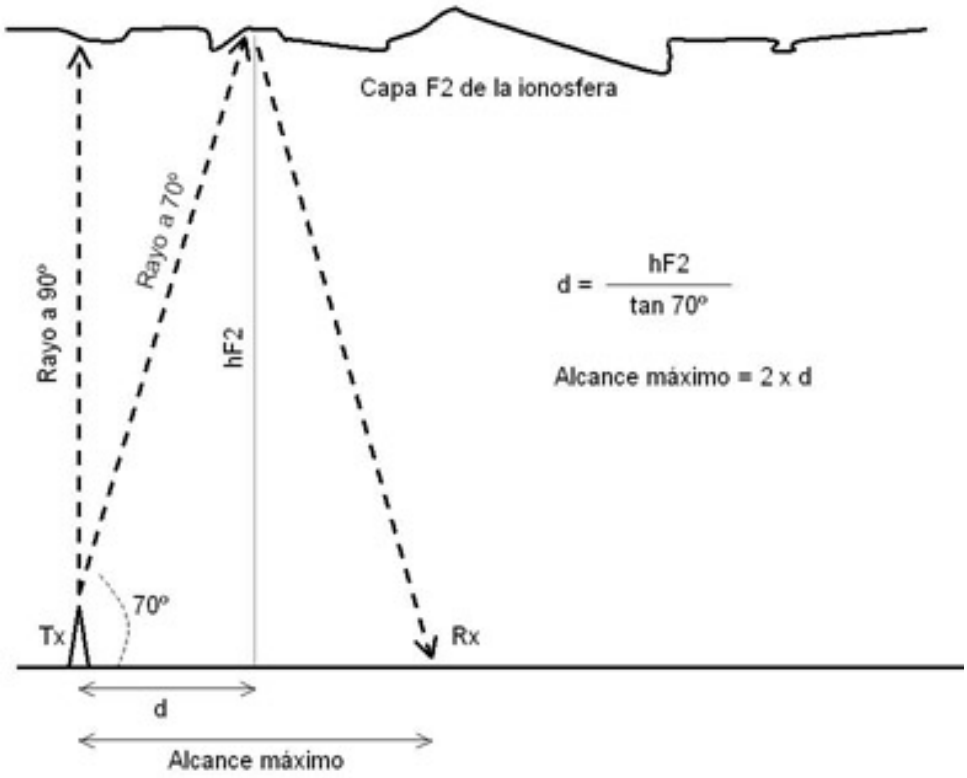

Figure 2.1: NVIS Communication example with the calculation of its coverage radius[5]

The figure above (Figure 2.1) shows clearly the radio-wave's path. The ray travels a certain distance until it reaches the ionosphere. Once there, it reflects in a specific layer of the atmosphere (the F2 layer in the image) and enables the communication between the two points (Tx and Rx in the image). The F2 layer and all its neighbours are explained in the following section to give more perspective on how the whole communication works.

2.2 The Ionosphere

The atmosphere is the famous and indispensable layer of gases that surrounds the planet on which we live. The gases at the top of it are the ones that are closest to the Sun and, due to solar radiation, they ionise. These ionised gases form a special layer within the atmosphere with some special properties, and it is known as the ionosphere. This layer, as explained in previous sections of this chapter, is responsible for the reflection that makes NVIS links viable.

If we study the ionosphere, the first thing we see is that it's several hundred km wide. This implies that the interaction of this layer with the sun is going to be different at the different altitudes that the gases within it present. These different heights and interactions an result in different gas composition and ionisation, respectively. There can be up to 4 layers, and their behaviour and appearance depends completely in then Sun's solar cycle and the hour of the day[6]. Specifically, and as can be seen in figure 2.2, during the day the ionosphere presents a total of 4 different layers (D, E, F_1, F_2) but during the night it presents only 2 layers (E, F). This phenomenon is completely logical because solar radiation changes significantly from day to night, thus changing the ionisation of ionospheric gases and, consequently, their behaviour[7].

The F-layer absorbs extreme UV radiation, with a peak at 175 km height. The E-layer, between 90 and 150 km height, absorbs soft X-ray and UV radiation. The D-layer, between approximately 60 and 90 km height, is responsible for high attenuation at the lower HF frequencies, and disappears almost completely at night.[4]

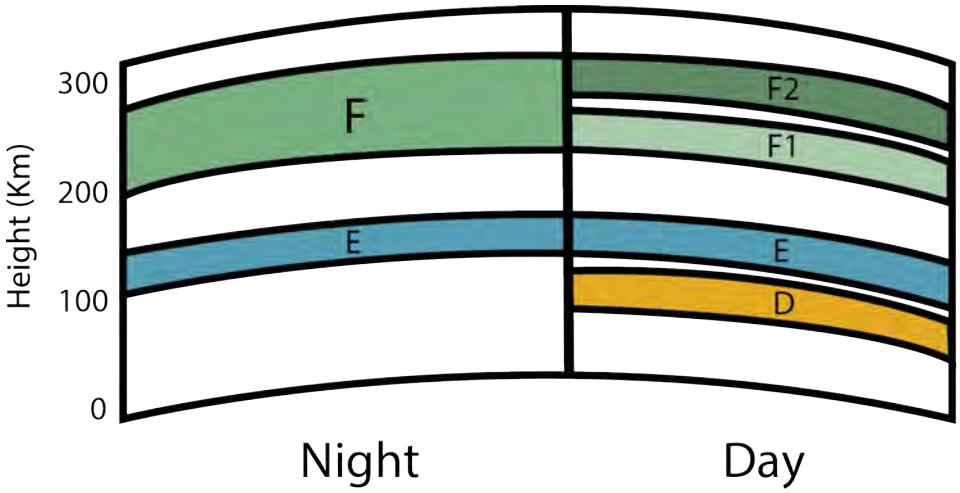

Figure 2.2: Ionosphere's layers throughout the day [7]

Figure 2.2 shows the different layers and their position throughout the day. As it can be seen, the F layer splits into two different sub-layers during daytime (layers known as F_1 and F_2, as the image represents). Of these two, the F_2 stands out, as it is the upper layer and also the one used to reflect the electromagnetic waves. this layer, therefore, is the one that determines the frequency that needs to be used in a NVIS link.

As introduced before, different frequencies signify different performances. If the near-vertical electromagnetic waves reach the ionosphere with a higher operating frequency than the critical frequency of the F_2 layer (frequency known as f_oF_2), the radio waves will pass through the layer at vertical incidence. Otherwise, rays with lower elevation angles will be reflected, resulting in the coverage starting at a certain distance of the transmitter while leaving a circular zone around the transmitter without coverage. This zone is known as the skip zone [4]. Figure 2.3 represents this zone, giving another graphical idea on how the NVIS links behave depending on the frequency band used.

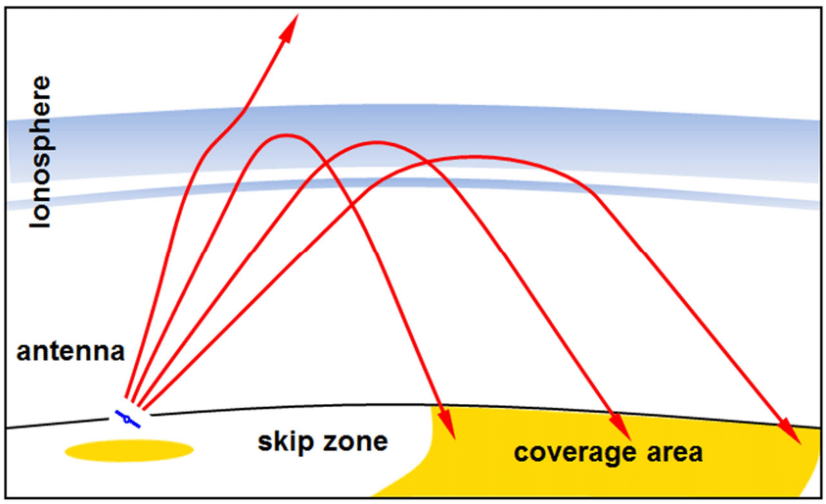

Figure 2.3: NVIS scenario with an operating frequency higher than f_oF_2 and different transmission angles [8]

NVIS communications aim to avoid the skip zone. To make this happen, the radio waves that enter the ionosphere must have an operating frequency lower than f_oF_2, so the electromagnetic waves will be reflected directly back to Earth (avoiding the creation of the skip zone). To sum up, it can be affirmed that to obtain a NVIS link with the correct coverage the frequency used must be below the critical frequency of the F_2 layer of the ionosphere. Figure 2.4 gives us an idea of a correct NVIS link without skip zone, an identical example of the link developed and studied in this project.

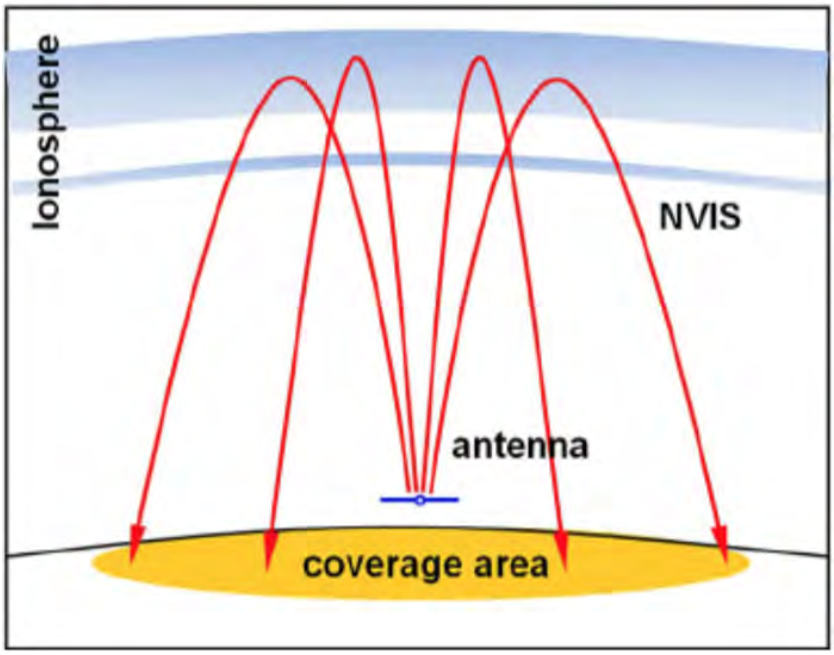

Figure 2.4: NVIS link[8]

2.3 Ordinary and Extraordinary Waves

Frequency election is key when a NVIS link is being developed. Previous sections of this document explained the main factors that needed to be taken into account, but there are two extra aspects to consider:Firstly, it is commonly known that the sun's rays variate throughout the day, having a maximum at mid-day and a minimum at the first morning hours, thus different frequencies should be used for day-time and night-time (being the nocturnal frequency lower than the diurnal frequency)[7]. Secondly, permanent links and scenarios need to consider not only the hour of the day but the sunspot cycle (with a duration of approximately 11 years).

The Sun is, then, one of the great protagonists of NVIS communications. It affects directly on the ionospheric reflection, which can be seen graphically in the images above (2.4). This reflection seems to return the same signal as the one sent by the transmitter but, in spite of this, the signal we receive when using a ionospheric link in a real-life scenario is not exactly the one we sent in the beginning. It has been mathematically proved that the radio waves that enter the ionosphere are split into two elliptically polarized characteristic waves due to the effects of the Earth's magnetic field. This two waves have the opposite rotation sense, and are know as the **ordinary** and **extraordinary** waves. This two waves suffer different attenuation and present different channel characteristics, as their path through the

ionosphere is different.[9]

This section is focused on the better understanding on how the two ionospheric characteristic waves are formed and how to benefit from them and their special properties.

The interaction of the Sun with the atmosphere can be grouped into three main points related to each other:

- **Solar Radiation and first effects:** The sun bombards the atmosphere from above, with powerful rays (mostly ultraviolet (UV) and X-Rays) that are absorbed when they hit atoms. These atoms split, and leave active and highly mobile electrons and larger less mobile charged ions. This effect defines the area of ionization, that extends from about 60km above the earth, out to about 500km.[9]

  This wide area has different properties, as it is commonly known that as the pressure in the atmosphere decreases with altitude, and so does air's density. This density reduction means a reduction of the number of atoms per unit volume. Also, the sun's effect over the atmosphere decays when we approach the Earth's surface. Figure 2.5 shows three graphs that indicate the different effects that the atmosphere suffers at the different heights of its ionization area.

- **Ionization:** When a radio wave reaches the ionosphere, the wave's electric field the electrons in the ionosphere into oscillation at the same frequency as the radio wave. Some of the RF energy is given up to this resonant oscillation. The oscillating electrons may either recombine, losing the radio energy, or will re-radiate the original wave energy[9]. The total refraction phenomenon can occur when the ion collision rate (recombination) is less than the radio frequency, and if the electron density in the ionosphere is great enough. That said, the mechanism is significantly complicated by differing ion density at different heights, and different chemistry involved in each refracting layer.[9]

  All this effect happens in all different heights of the ionosphere. Despite that, there is a point where there are a high number of atoms with a remarkably high radiation, resulting in a peak in the level of the ionization of the atmosphere. This peak can be seen in the third graph of Figure 2.5, peaking at about 300km. The first and second graph of Figure 2.5 show, respectively, the atmosphere's gas density in relation to height and the radiation intensity in relation to height.

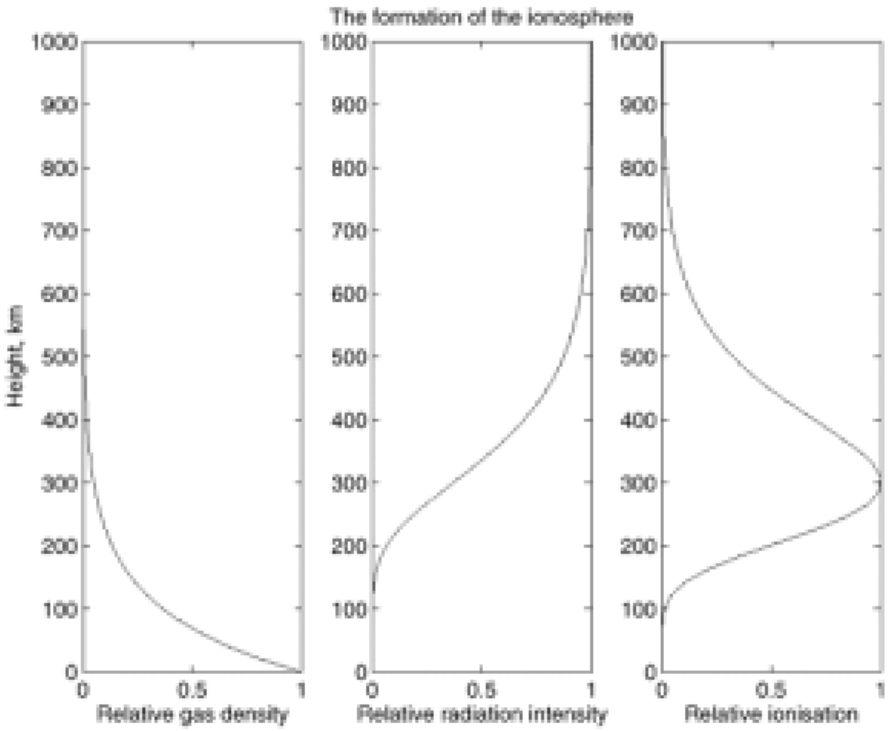

Figure 2.5: Ionosphere's formation informative graphs[9]

- **Refraction:** The refraction phenomenon occurs because the atmosphere's ionized molecules present free electrons, which vibrate in response to the radio signals reaching them. The behaviour of each of these moving electrons resembles small dipole antennas.[7]

Figure 2.6 shows a graphical approach of the movement of the electrons and their behaviour when a radio wave reaches them. This spinning results in a polarization change for the incident radio wave. Furthermore, waves of different polarization can be refracted different amounts. This leads to the return to earth of two different rays with distinct properties, waves known as the Ordinary and Extraordinary rays. Just as with reflections from other layers or at other times, these rays can have slightly different frequencies, phase, amplitude and time of arrival[9]. This different properties can be used in order to improve telecommunication links, as polarization diversity techniques are an option in ionospheric channels.

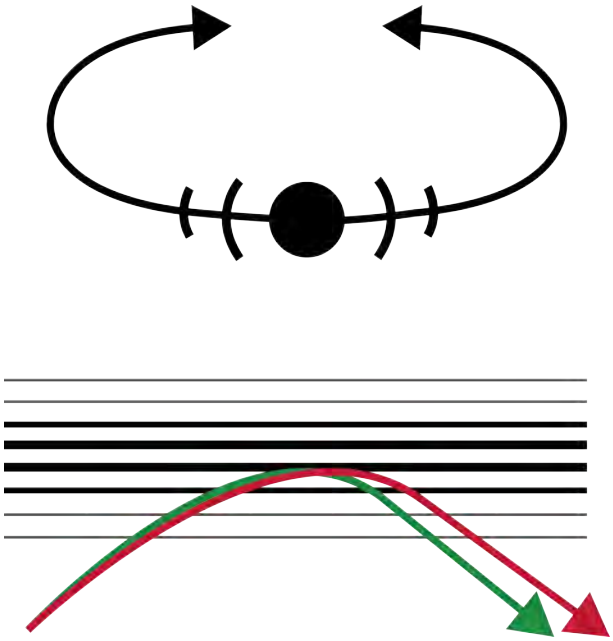

Figure 2.6: Electrons vibrating in the ionosphere and refraction[7]

2.4 Channel Parameters

When studying a telecommunication channel, some parameters affect directly the performance of the link. Understanding this parameters is fundamental in order to minimise the errors in the link (less Bit Error Rate (BER)) and maximise the data throughput. All the channel parameters defined below have been taken into account when designing the overall system and the frame, all in order to improve the link's behaviour.

Coherence Time

The coherence time is defined as the interval within which the channel has a statistically similar behaviour[10]. Specifically, it refers to the time during which the variations suffered by the channel do not alter the transmitted signal. This time usually goes related to the Doppler Spread[11]. This parameter will force us to have a signal time and length inferior than the ionosphere's coherence time.[7]

Doppler Spread

The Doppler Spread is inversely proportional to Coherence Time, and it also is a parameter that measures the variability of the channel. Actually it measures the speed of variation of channel behaviour, and it corresponds to the frequency range of the Fourier transform transmission in the time domain of the autocorrelation function of the non-zero channel impulse

response.[12]

Doppler Shift

This parameter is more commonly known as the Doppler effect. It is the variation of frequency of a wave between its transmission and its reception. This frequency variation is due to the relative movement between the transmitter and the receiver, which in our scenario is produced by the displacement of the physical layers of the channel (the ionosphere).[7]

Also, the modification of the signal can generate distortions in the reception, which can be both constructive or destructive depending on the phase that brings this modification of the frequency. Another possible source of Doppler Shift is the difference between the transmit and receive sampling frequencies. This parameter needs to be corrected in order to decode the signal correctly.[7]

Multipath

Multipath is an important parameter to take into account when designing the communication system. Radio waves emitted by the transmitter travel different paths due to the environment of the scenario and, therefore, arrive at different moments to the receiver. This is measured with the "Delay Spread", interpreted as the time difference between the first wave (of the first shortest path) and the last wave (longest path) that arrives in reception of the same transmitted symbol.[7]

In order to avoid interference in a link (avoid ISI, Intersymbol Interference), the transmitted symbol's time has to be correctly designed in order to reduce the difference between the first and last component of the multipath.

Fading

The fading is the loss of power (also known as attenuation) between the transmitted signal and the received one. When using the ionosphere as a channel, this fading is always present due to the interferences that appear from the different signals that arrive from different paths (as the transmitted signal reflects in different layers of the ionosphere).[7]

2.5 Polarization Diversity

The implementation of polarization diversity via the use of dual-polarized antennas is a promising cost and space effective alternative, where two spatially separated uni-polarized antennas are replaced by a single antenna structure that employs orthogonal polarizations

[13]. This project shows the study of polarization diversity in a SIMO link even though MIMO systems are the ones that benefit most from systems based on polarization diversity. Future research should focus on developing a MIMO link where polarization and also spatial diversity work hand-to-hand in order to improve both robustness and capacity of a certain scenario. In our case, using the SIMO mechanism together with polarization diversity results in lower transmitting powers and, therefore, lower consumption or antenna dimensions (very interesting in remote sensing networks).

This diversity technique has already been applied to HF, radar, and imaging systems, and has demonstrated its potential for improving the capacity of wireless communications systems[14]. This improvement is typically granted by an additional decorrelated channel provided by an orthogonal polarization state to the existing one. In this project's case, the Ordinary and Extraordinary waves are the two orthogonal channels under study.

When studying polarization diversity links, the cross-polarization discrimination (XPD) factor is the usual evaluating parameter, with low correlation coefficients being achieved even in NLOS (Non Line of Sight) situations [14]. When high correlation coefficients are measured, or even with decent correlation coefficients, spatial diversity is the main alternative to take into account. That said, since at least 20λ horizontal and 15λ vertical separation distances are required for efficient spatial outdoor diversity in practice (resulting in a separation of tens of meters between antennas), polarization diversity is the most coherent solution.[14]

As said before, the idea of polarization diversity is based on an additional decorrelated channel with an orthogonal polarization to the existing one. NVIS communications can benefit from this diversity technique because, as the first section of Chapter 3, two characteristic wave components with circular polarization of opposite sense appear, each component following a different path through the ionosphere, when a radio wave of certain frequency reaches the ionosphere.

The effectiveness of both diversity reception and HF MIMO increases with decreasing correlation between the received signal streams. In our study, these streams are the two characteristic wave components with circular polarization of opposite sense, each following a different path through the ionosphere. If the natural decoupling between both characteristic waves is sufficiently large and if it can be put to use, this will drastically improve HF MIMO and diversity reception[4]. Figure 2.7 shows a measurement of the two characteristic waves and their isolation throughout different hours of the day, confirming the viability of polarization diversity for NVIS systems.

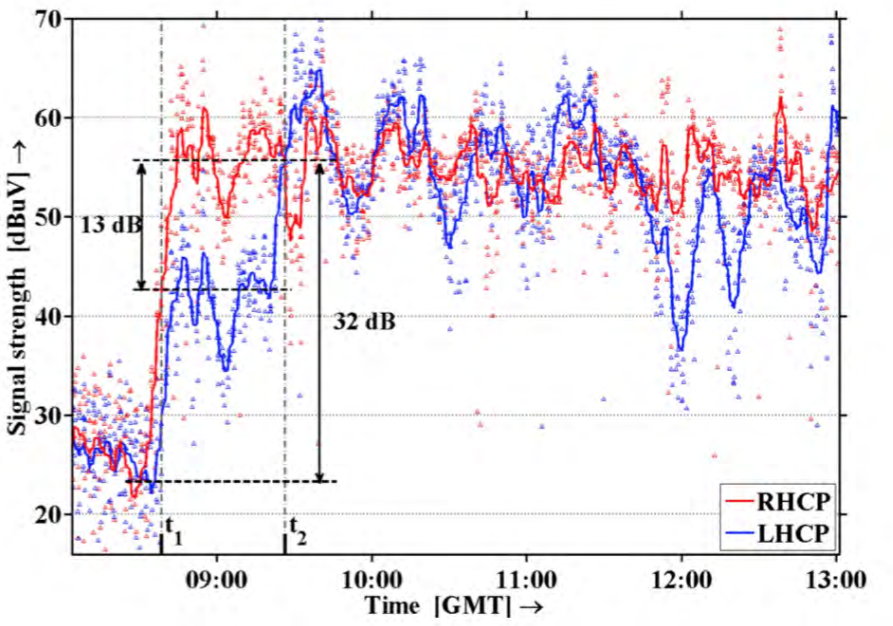

Figure 2.7: Measured LHCP and RHCP signal strength and Channel Isolation[4]

For HF MIMO, the use of LHCP and RHCP antennas at the transit side and at the receive side would create two very well isolated channels, maximising MIMO gain[4]. Despite that, in the study done in this project the transmit antenna will be a linear polarized one, leaving the MIMO studies with LHCP and RHCP antennas for further research. Figure 2.8 shows the decorrelation between the two ionospheric channels, one of the results obtained in a study carried out in 2019 on a link very similar to the one used in this project. This decorrelation is bigger than the one displayed, as the three curves represent the mean values of each hour. If every frame received would be compared, a bigger difference of E_b/N_0 would appear on the graph.

Three curves can be seen in the figure above (Figure 2.8). The acronyms used are: SC for Selection Combining (a diversity combining technique, which will be explained in the next section), X for the extraordinary channel and O for the ordinary channel.

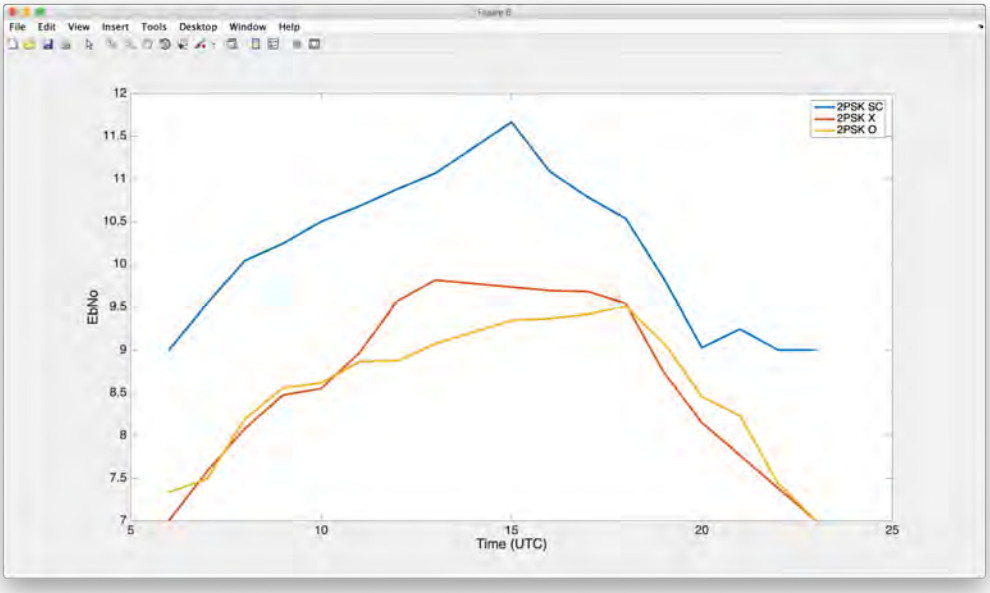

Figure 2.8: Overlapped 2PSK results for a Barcelona Cambrils NVIS link, E_b/N_0 vs Time Graph[7]

2.6 Diversity Combining Techniques

Diversity has long been recognized as an effective technique for combatting the detrimental effects of channel fading [15]. Many diversity techniques have been used during the years in order to improve telecommunications. The most popular ones are: Time diversity, Space diversity, Frequency diversity, Multiuser diversity, Cooperative diversity and, just as in our study, Polarization diversity. All the diversity techniques mentioned need a process of combining the different signals that arrive at the receiver. This combining techniques are called Diversity Combining Techniques. Technically, Diversity combining is the technique applied to combine the multiple received signals of a diversity reception device into a single improved signal[16].

Firstly, a new term has to be introduced in order to understand the diversity combining processes: the Diversity Gain. This new parameter is the increase in signal-to-interference ratio (SNR) due to some diversity scheme, or how much the transmission power can be reduced when a diversity scheme is introduced, without a performance loss. Diversity gain is usually expressed in decibels, and sometimes as a power ratio[17]. This term won't be calculated on the measurements of this project, but it helps understand the fact that there will be an increment in the SNR of the signal received when using a diversity combining technique (Figure 2.8 gives an early idea about this gain, a result that was obtained with a

similar link than the one used in this study).

There are some different ways to combine the signals, and all follow different processes. This project focuses and uses two different methodologies:

- **Selection Combining (SC)**: Technique that, as it name indicates, selects one signal of the N input signals. Of all the received signals, the strongest signal is selected. Figure 2.9 shows a graphical idea of the performance of the Selection Combining Method with two input branches.

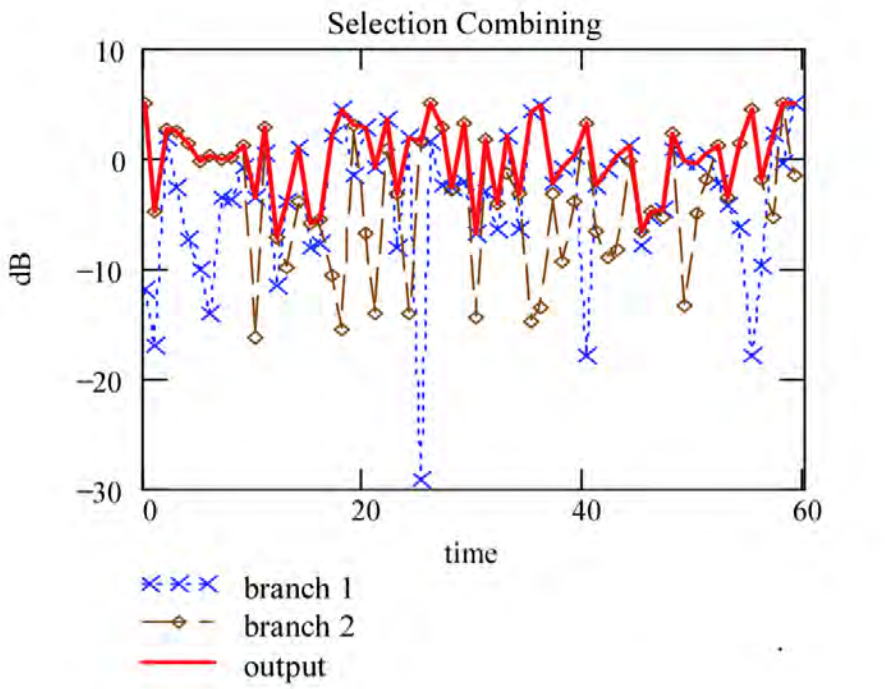

Figure 2.9: Selection Combining process output [18]

- **Equal Gain Combining (EGC)**: Method that coherently adds all the signals received, without applying any weighting process. Figure 2.10 shows a graphical idea of the performance of the Equal Gain Combining Method with N input branches.

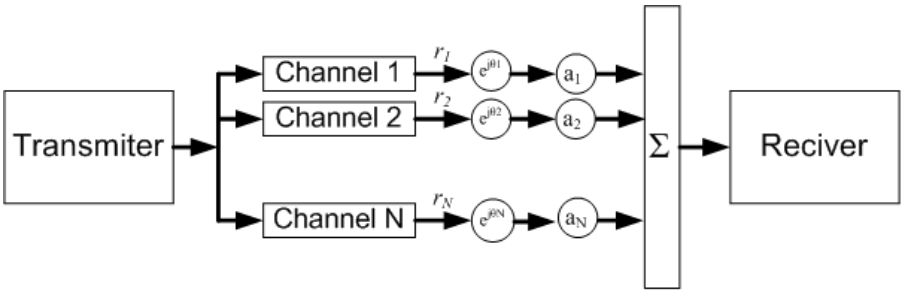

Figure 2.10: Equal Gain Combining process[19]

Another combining technique that seems a candidate in our project is the Maximum Ratio Combining (MRC). This method gathers all the signals received, weights them with respect to their SNR and then it sums all the waves. This technique is often used in large phased-array systems and has been discarded as our system only has two different branches.

2.7 Digital Modulations

The modulations used are one of the main aspects of the whole study. Of all the possible modulations, three digital ones have been chosen for this work. The whole study of our scenario will be based on the performance of this modulations, scanning them with different transmitting power values.

As for the modulations used, we find the PSK (Phase-Shift Keying), FSK (Frequency-Shift Keying) and QAM (Quadrature Amplitude Modulation). Regarding the modulation orders, modulations from order 2 to order 32 have been tested. It should be noted that increasing the order of modulation decreases the E_b/N_0 of the signal. This parameter is more important than the SNR, since in this case it indicates the bit energy with respect to the noise.

Furthermore, it has to be taken into account the symbol positioning in the IQ diagram in the QAM and the PSK modulations. For both PSK and QAM modulations of orders 2 and 4, the symbols have been placed in a particular way in the IQ diagram in order to study different aspects of the transmission. Firstly, the order 2 modulations have different constellations for the 2QAM and the 2PSK. In this study we wanted to test the efficiency of 2PSK with its two symbols on the real axis of the IQ diagram. On the other hand, the 2QAM has been tested with its symbols on the real and imaginary axes. The purpose of this constellations, is to test which modulation is more efficient: one on a single axis or one using both real and imaginary axes. Figure 2.11 plots the IQ diagram of the 2QAM and 2PSK modulations

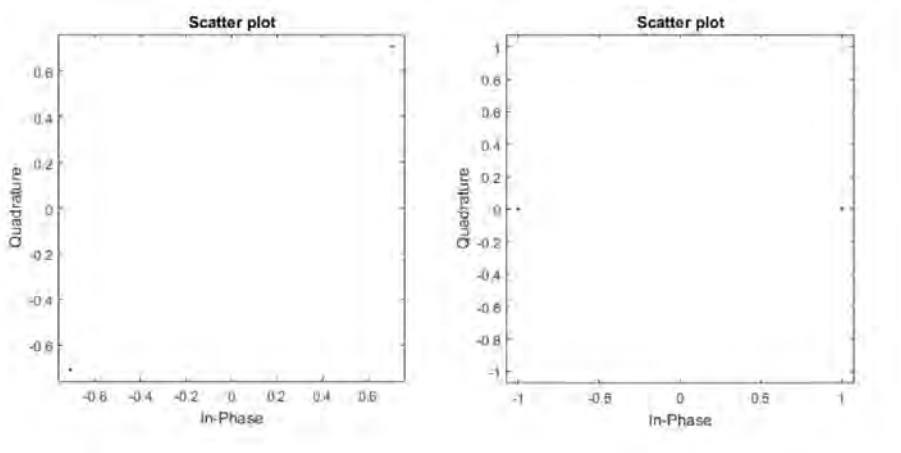

Figure 2.11: 2QAM (left) and 2PSK (right) constellations [20]

Regarding the 4QAM and 4PSK modulations, the constellation has been designed and implemented identically between them. The 4 symbols are split 2 and 2 on the real and imaginary axes, as Figure 2.12 shows. This positioning has another specific purpose, which is to study the behaviour of the channel coherence time and its meeting with different modulation orders and to verify the results obtained with the order 2 modulations (related to axis independence). Both assumptions and comparisons were verified and studied by J. Porte, J.M. Maso, J.L. Pijoan and D. Badia during the 2018 - 2019 academic year. [21]

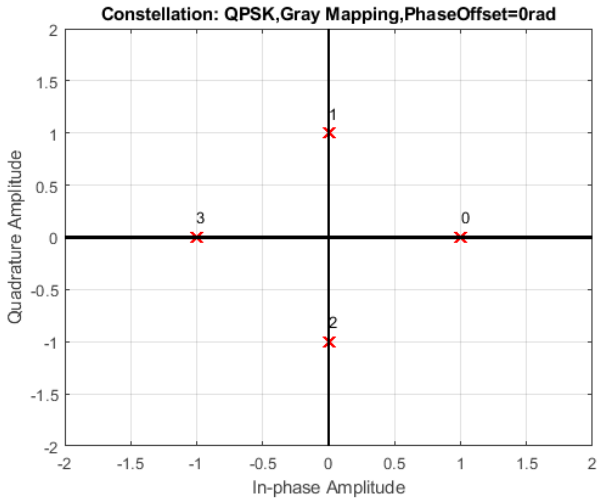

Figure 2.12: 4QAM and 4PSK constellation [22]

For higher order modulations, constellations imply lower E_b/N_0 but can transmit a large number of different symbols. The study presented in this project uses modulations of 5

different orders, ranging from order 2 to order 32. High order QAM and PSK modulations present close symbols and very complex constellations. The following figure indicates the constellations used for the QAM modulations sent in our scenario.

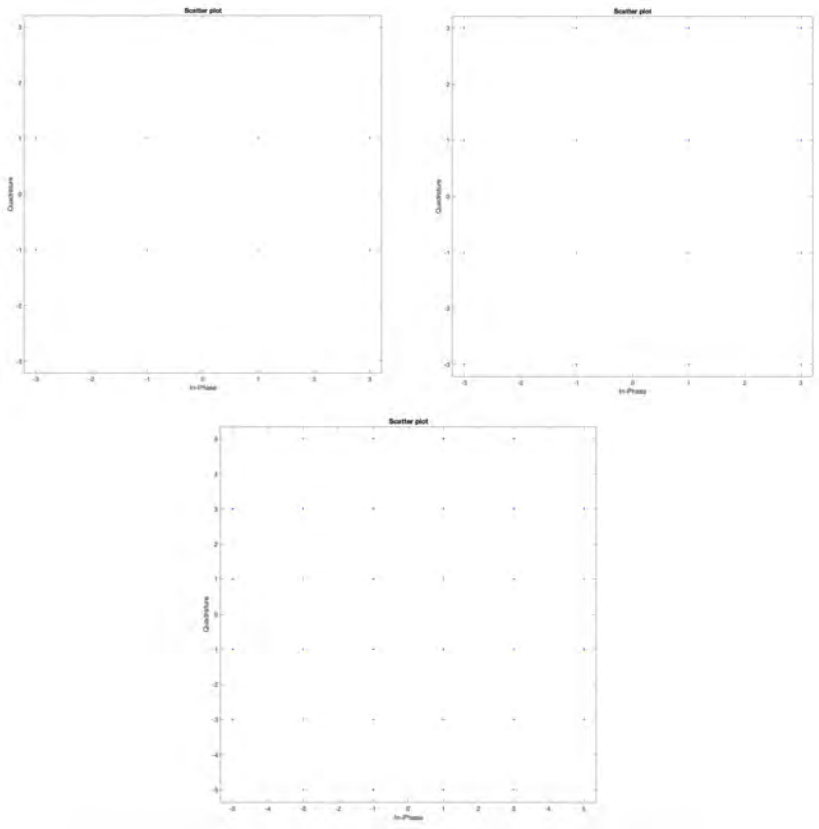

Figure 2.13: 8QAM, 16QAM and 32QAM constellation

Chapter 3

Experiment realization

This work is focused in the deep study and improvement of a NVIS link in order to be able to upgrade future telecommunication systems based on the same technology. The use of the ionosphere's properties, its two characteristic waves and their respective polarization have still new horizons to discover despite having been already used in other projects [7] [4]. This Chapter explains the infraestructure needed to realize the polarization diversity experiment with a complete power and modulation study.

3.1 System Description

The main objective of the designed and performed tests is the analysis the behaviour of the ionosphere's ordinary and extraordinary waves when studied concurrently through a NVIS channel. Furthermore, the scenario implemented requires a scan of both characteristic waves simultaneously, forcing the application of polarization techniques in order to improve quality of the demodulation of the frame and, therefore, the link's results. For that purpose, the system that has been assembled to perform the deep study of the ionospheric channel is based on a configurable sofware defined radio platform.

The main weakness of using the ionosphere as a communication channel is the amount of negative effects that our signal transmitted suffers. Having the necessary hardware and software to mitigate these effects is a prerequisite for any link that uses the NVIS communications channel itself. As technology is continuously improving, new digital gadgets and algorithms make this complex process of solving the ionosphere's vulnerabilities become less costly and more efficient.

The platform that has to be developed for scenarios like the one in this project has even more challenges. Two main aspects to be taken into account and that have to co-exist are that the platform must be able to implement and study all the different tests and hypotheses and, at the same time, has to allow the designed tests to be performed and validated.

All this needs and objectives can be accomplished with a single device, specifically a Field-Programmable Gate Array (FPGA).

To achieve the different objectives presented and to develop a low-cost platform, the STEMlab 125-14 board hardware has been chosen, product from the manufacturer Red Pitaya[23]. The hardware's main core is a Zynq-7010-SOC [24]. These products can contain a one-core or two cores (depending on which product is chosen) ARM® CortexTM-A9 [25], based processing system (PS), plus 28 nm of Xilinx programmable logic (PL). In addition, this board has different peripherals that allow the user to develop a robust platform for remote sensing [3]. Figure 3.1 shows the hardware used, including the FPGA and the different peripherals utilized. Below the image, an explanation of each of the devices and infrastructure used is given.

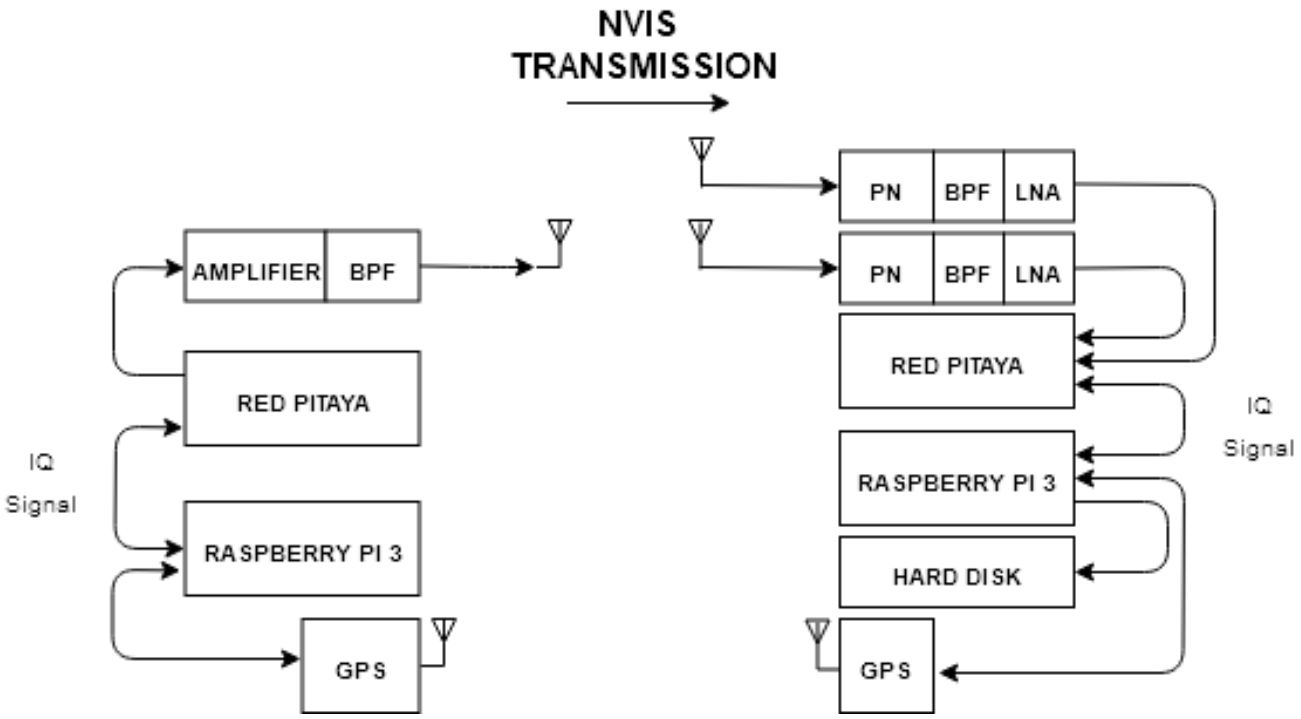

Figure 3.1: Schematic of the remote sensing platform [3]

Zynq (FPGA/Cortex)

The FPGA is essentially dedicated to data processing and the Cortex to time and data management. In reception, this module allows the the reception and processing of the received signals in the analog to digital converters (ADCs). This data is then sent in real-time to the Cortex via direct memory access (DMA). When the information reaches the Cortex, the

information is written on an external hard disk. On the other hand, in transmission, the Cortex contains the information that will be sent to the FPGA to be transmitted.[3]

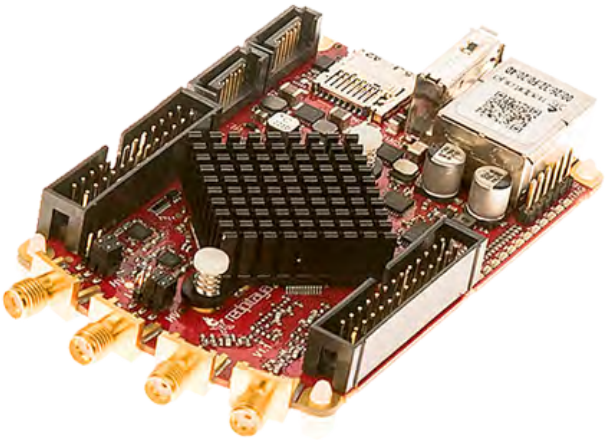

Figure 3.2: RedPitaya kit with a Zynq-7010-SOC processor [23]

Converters

This project relates two different worlds from the engineering field. Both analog and digital signals are transformed, studied and treated. To change from one type of signal from one kind to the other one, a specific converter is needed. Specifically, the board used has two channels, with two analog digital converters (ADCs), with a resolution of 14 bits and a sampling frequency of 125 MSPS. These, along with the two SMA connectors, allows the reception of a signal by the used antenna, the sending of this signal to the FPGA and, finally, the treatment the signal. Additionally, disposing of two independent ADCs allow us to receive both ordinary and extraordinary waves at the same time[3]. This parallel study will also allow us to make a fair comparison with all the different polarization techniques.

If we study the transmitter, it has the opposite function to the one implemented by the ADCs. For the system to work properly we need the transmitter to take a digital signal and transform it to an analog signal, which will come out with an antenna later. Digital to Analog converters (DACs) fulfill our purpose of bringing one digital signal to the analog world. Therefore, this peripheral is only used by the FPGA [26].

RaspBerry PI-3

A second post-processor is present in the system. A Raspberry Pi-3 communicates with the main core via Ethernet to control peripherals, save the received frames correctly (in reception) and prepare the sent frames (in transmission). The objective of this secondary core is

purely related to raw data and frame design.

When transmitting the data, the Raspberry disposed of a file with a tone and PN sequence, which will be saved on an array. The data that wants to be transmitted is modulated and, afterwards, it is gathered together with the array that contains the tone and the PN sequence. Finally, the array is sent to the RedPitaya[11]. When receiving the data, the RedPitaya board sends it to the new core (the Raspberry), device that will collect all the data in order to process it later with a Data-Processing software. Matlab has been the software used in this study.

Figure 3.3: Raspberry Pi 3 used in both transmitter and receiver [27]

Antennas

All wireless communications share a common and, at the same time, indispensable device: antennas. Antennas depend completely in the frequency band use and can occupy from a few millimetres of space to tens of meters. As the study carried uses the HF band (3 - 30MHz) and the antennas are always of dimensions proportional to the used wavelength (λ), the magnitudes of the antennas used in the system have been considerable, reaching tens of meters high and wide [7].

Our scenario disposes of a total of three identical antennas. One of them is the one responsible of the data transmission and is located in Barcelona (in the La Salle Univeristy Campus), while the two remaining are the ones in charge of the data reception and are located in Cambrils (in the La Salle's Sant Josep house). Figure 3.4 shows a picture of the transmitting antenna located in Barcelona, while Figure 3.5 shows a photography of the two receiving antennas in Cambrils. The antennas used have been highlighted for a better understanding.

Figure 3.4: Transmitting antenna in Barcelona. Inverted vee antenna made of a flat copper, tunned at 5.4MHz and located in La Salle's Campus. [7]

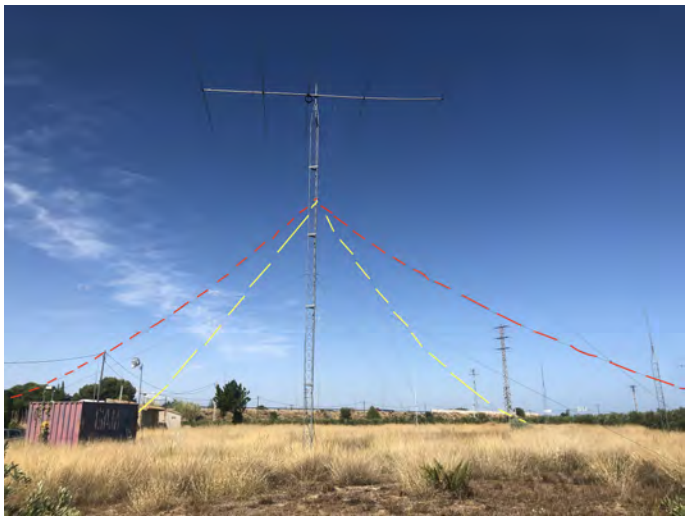

Figure 3.5: Reception antennas in Cambrils. Two inverted vee antennas made of a flat copper, positioned orthogonally, tunned at 5.4MHz and located in Sant Josep's of La Salle. [7]

The three antennas of the experiment are completely identical. All three are made of a flat copper conductor in the shape of inverted Vee, and are tuned to the frequency of 5.40 MHz[3]. The choice of the antenna design (inverted Vee) has been based on three main points: firstly, they are easy to build and install as they only need a mast and, secondly, their gain is similar to the horizontal dipole. Finally, they are ideal for NVIS links as they have a good radiation pattern in upwards direction.[3]

The frequency (5.40MHz) has been chosen and calculated from the revised ionograms of Observatori del Ebre[28], a frequency lower than the cutoff frequency that allows us to correctly receive ordinary and extraordinary waves from the ionosphere[3]. Additionally, earlier studies with other frequencies [7] have also influenced in the frequency election. The frequency is chosen based on the ionosphere's reflection, as it is desired to have the minimum losses possible. Concretely, and thanks to the deep ionogram study and the fact that the ideal frequency is 10 % less than the critical frequency F2 [29], the 5.40MHz frequency has been the final election.

The transmitter used in the scenario is remarkably less complex than the receiver. The reception part of the scenario is more sophisticated as our experiment follows a Single Input Multiple Output (SIMO) design, having only one antenna in transmission and two antennas in reception, which are set perpendicularly. This configuration together with a phasing network that delays one antenna to the other will allow the system to receive different polarizations simultaneously, which is the main goal of the scenario itself.[3]

The Phasing Network

Circularly polarized antennas are needed in order to accomplish the polarization diversity objectives of this research. Added to the linear-polarized antennas, a phasing box has been designed and implemented. This hardware realized the desired delays with a combination of coaxial delay lines. To be more specific, the box gets 2 inputs, one per antenna. This 2 inputs are split into a total of 4 signals (2 signals per antenna) with a radio frequency splitter. This four signals are the ones that our box will treat in order to modify the polarization of the antennas. The paths of the two antennas is the same, and it is the following one: one feed line is connected directly to a RF Combiner, and the one cable is lengthened with a quarter wave phasing line to provide 90° phase shift. The output of the box gives us a phase difference between the dipoles antennas of either +90° and -90°. For the designed system, the phasing network is for one single frequency. For a multiple frequency receptor, the phasing network should be done in digital[7]. Figure 3.6 displays a block diagram of the phasing network used in the experiment. Figure 3.7 shows a picture of the physical implementation of the phasing box.

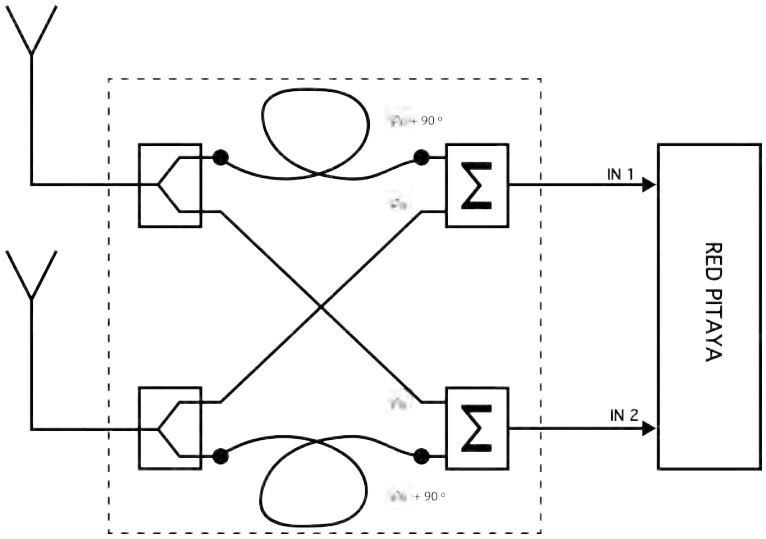

Figure 3.6: Block diagram of the phasing network[3]

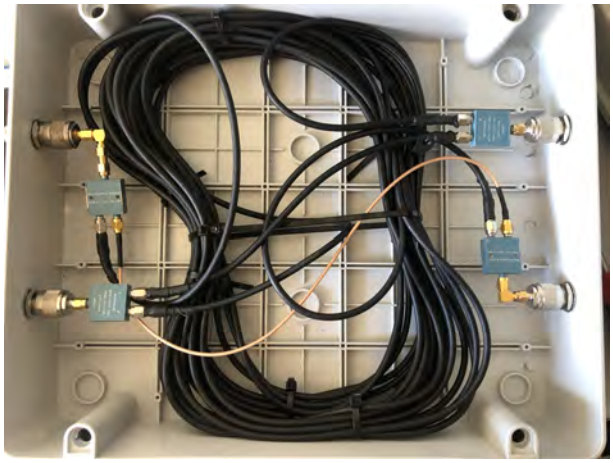

Figure 3.7: Physical implementation of the phasing network[7]

The phasing network's objective is to unify the two orthogonal linearly-polarized antennas so that two circularly polarized antennas are created. Mathematically, the polarization vectors of the resulting antennas are developed below:

$$LHCP_{Antenna} = \hat{x} + j \cdot \hat{y} \tag{3.1}$$

$$RHCP_{Antenna} = j \cdot \hat{x} + \hat{y} \tag{3.2}$$

Equation 3.1 belongs to the Left-Hand Circular Polarization (LHCP), while equation 3.2 belongs to the Right-Hand Circular Polarization. As this research has been performed in the northern hemisphere, it has been studied and demonstrated that the LHCP corresponds to the ordinary wave and, respectively, the RHCP is related to the extraordinary wave[4].

Amplifier

Our study is based on a power sweep from 3W to 100W using three different modulations of a total of 5 different orders: FSK, PSK and QAM modulations. As we transmit non-constant envelope modulations (QAM) using a class A amplifier is a must[3]. Despite the maximum testbench power transmission is 100W, an amplifier of 250W has been installed and used in the transmitter.[3]

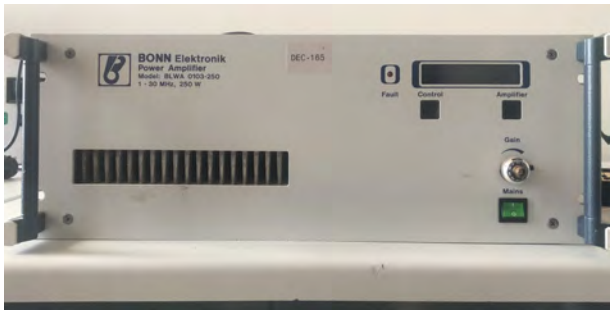

Figure 3.8: HF Power Amplifier, Model BLWA 0103-250 used in the transmitter[7]

Filters

The link implemented has several Band Pass Filters (BPF) situated strategically all over the platform. There are two different BPF in the scenario. The first ones, located in the transmitter, are a band HF band-pass from the 3 MHz to 7 MHz, as this frequency range is defined for the NVIS channel. The second ones, are defined from 4 MHz to 6 MHz, and have the objective of filtering possible interferences in the receiver.

The filters present an attenuation of 0.7dB in the passing band. The lower frequencies (frequencies below 3MHz and 4MHz, depending on which filter) are abruptly attenuated, with an attenuation value of approximately 70dB in the 2MHz frequency. This design is based on the high amplitude values of the AM signals that are next to our band. On the other hand, the upper frequencies are not as abruptly mitigated. The attenuation value of them is approximately 40dB in the 8MHz frequency.

GPS

The synchronization in time between the transmitter and the receiver is accomplished via GPS [3]. This GPS is clue in the transmission and reception process, as the data is transmitted exactly every minute. This peripheral is connected to both TX's and RX's Raspberry Pi 3. This module is fundamental as the infrastructure used is low cost and needs a second peripheral just to accomplish the synchronization between the TX and the RX sides.

Post-processing data

The data received by the system needs a processing. This processing is done via software, and it has been realized with the Matlab software [30]. Matlab has been the tool used to both demodulate all the tests frames received and obtain the results and graphics in this document.

The data processed has been the following: A total of 4130 files of 29,7Mbytes each, resulting in more than 122 Gbytes of data to process. The data processed is just limited by the capacity of the hard disks in reception handled by the Raspberry Pi-3, these having a capacity of 128Gbytes.

3.2 Tests performed

This section of the document is focused on the detailed explanation of both the scenario where the tests were performed, the frame designed of the signals transmitted in these tests and the tests themselves.

Scenario

The research in this project and its tests were carried out in the Catalonia region in Spain, where a link between two distant NVIS nodes was established. As previous sections mentioned, the transmitter node was located at La Salle University - URL on Barcelona, while the receiver node was situated in the city of Cambrils (Tarragona region, Spain). Figure 3.9 shows a satellite picture of the terrain, with the node locations marked in red. The distance between the two points (withoud Line of Sight (LOS)) is approximately 96km.

Figure 3.9: Near vertical incidence skywave (NVIS) test link [3]

In previous sections of this chapter (Figure 3.5 and Figure 3.4) the inverted Vee antennas installed are shown. The transmission has been established in Barcelona and the reception in Cambrils. This choice is not random, and it is based on the high interferences and electromagnetic noise at the HF band in Barcelona and its surroundings.

The tests performed have been taken for 15 days between the 7 of December to 22 of December of 2019. The frames have been transmitted every minute during these days [3].

Frame Design

The frame transmitted is one of the most relevant points of the study in order to achieve the expected results in the tests performed. Every test in this work consists in the transmission of previously designed frame. Figure 3.10 shows a graphical approach of the tests' frame. Every frame is composed by a total of 50 packets, each one of them mainly formed by data of the three different digital modulations studied in this project (QAM, PSK and FSK). The raw data is not the only information inside the frame. The frame designed has three main parts with different functionalities: 600 Hz Tones, PN Sequences and the modulations' data itself. Precisely, every modulation is preceded by both the tone and the PN sequence in order to mitigate most negative channel effects and synchronize the system [3].

Figure 3.10 also clarifies the length and properties of every data block. Each block contains a total of 250 symbols with a resampling of 42 (10500 samples divided by 250 symbols), resulting with 2.3kHz of bandwidth. Apart from the data, another important aspect to take into account when designing a frame is the time of each packet. This time was carefully chosen in order to fulfill the coherence time requirements of the ionospheric channel [31].

The most restrictive coherence time studied in the ionosphere until the experiment was 1.46 s [32]. To accomplish a good and bulletproof design, the time of the experiment's frame was set at 510.36 ms. In order to compare correctly the effects of the ordinary and extraordinary waves to the modulations transmitted, it is fundamental to transmit every packet in

the coherence time marked[3]. The total duration of the 50 packets is approximately of 25 s.

The frame and its design works hand to hand to the post processing of the data. When studying the data after performing the tests, the following process is followed for each frame: Once the system identifies the frame, the first block encountered is the 600 Hz tone. This tone of a duration of 60 ms is key to correct the Doppler shift, negative aspect of the channel that affects the rest of the block[3]. This Doppler shift comes mainly from the Red Pitaya platform clocks, which have a low stability and create Doppler shift effect higher than the ionospheric. Measures of the platform show that the maximum value of the Doppler shift received due to the low stability clocks is about ± 20 Hz. The 600 Hz tone added to the frame helps identifying the Doppler shift inserted by its variations between 580 Hz or 620 Hz. Worst case scenario, if a received tone frequency of 580 Hz is considered, the measure could be done with 34 cycles (60 ms). If we make use of a DC constant instead of a 600 Hz tone, the measure will be done with the 16th part of a cycle (60 ms), which is not enough to take a real measure.[3]

The second auxiliar block included in the frame is a 6th order PN sequence, which is used to synchronize with the modulations data inside the transmitted signals. The resampling of the PN sequence is about 8 and has a total duration of 5.12 ms[3]. The order and duration of the PN sequence have been carefully designed, studied and tested to mitigate the channel effects of Doppler shift, Doppler Spread and delay spread.

The modulated data blocks are located just after the PN Sequence. These blocks are the main focus of the research, as they are transmitted, received and studied with different polarization techniques, modulation and transmitting power values. Specifically, and as mentioned earlier in this report, the tests performed, have been done with three different modulations (PSK, FSK and QAM) with different modulation orders between 2 to 32 for power transmissions between 3W and 100W.

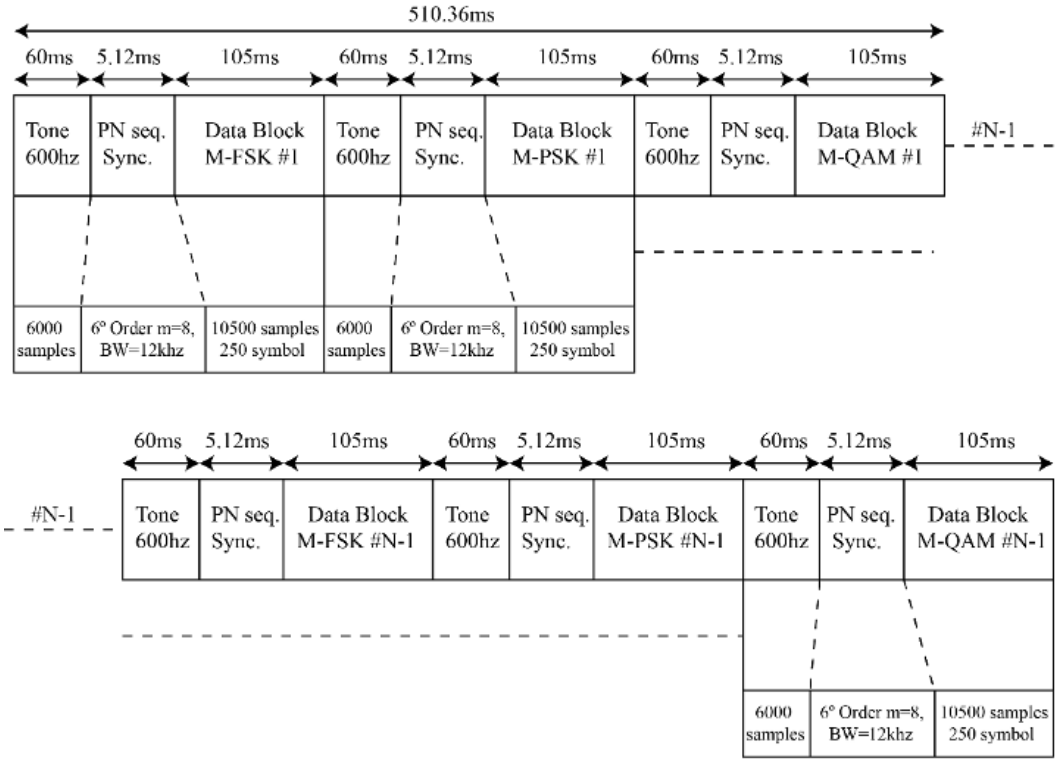

Figure 3.10: Frame design and properties [3]

Notwithstanding the process explained, an extra block must be added to the frame for the initial recognition of the transmitted data. This block precedes the first tone of the frame and consists on a PN sequence. This PN sequence, as well as the others, has the purpose of synchronizing the system and preparing the receiver for the incoming data. Figure 3.11 shows a block diagram to complement the explanation and understanding of the frame.

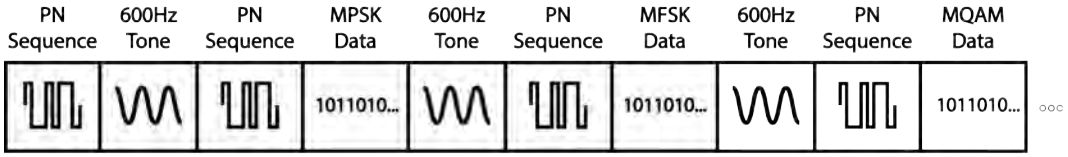

Figure 3.11: Block diagram of the Frame [7]

Testbench

Previous work opened the doors to SIMO communications and diversity techniques in NVIS links [7]. This project presents a much deeper study as this section will expose. A complete

testbench has been designed in order to get complete results and perform all the tests needed in order to have a solid vision of NVIS polarization diversity scenarios, opening even more new horizons for further research.

In order to perform a complete power sweep, power transmissions between 3W and 100W appear in the testbench designed. Furthermore, the modulation study is also present in the testbench, appearing with order modulations between 2 to 32, with a bandwidth set to 2.3kHz and using a total of three modulations: PSK, FSK and QAM. After running all the tests and obtaining the results, signal-processing algorithms in Matlab have been carried in order to obtain the graphics shown below. The software developed is the one that applies the diversity combining techniques and analized the polarization of the signals received. Table 3.1 displays all the tests performed in one hour of transmission. A total of 25 tests with different modulations, modulation orders and transmitting power are carried out.

Order of Modulation	**Power Transmission**	**Minute**
2, 4, 8, 16, 32	3W	05, 06, 07, 08, 09
2, 4, 8, 16, 32	6W	15, 16, 17, 18, 19
2, 4, 8, 16, 32	12W	25, 26, 27, 28, 29
2, 4, 8, 16, 32	25W	35, 36, 37, 38, 39
2, 4, 8, 16, 32	50W	45, 46, 47, 48, 49
2, 4, 8, 16, 32	100W	55, 56, 57, 58, 59

Table 3.1: Testbench transmitted

Chapter 4

Measurements results and observations

This chapter analyses the most relevant results obtained from the performed tests. The ordinary and extraordinary waves and their influence in the modulations performance, the Bit Energy to Noise Power spectral density (E_b/N_0) and the effectiveness of the polarization diversity techniques in order to improve as much as possible the NVIS link established. All the graphs have been computed and obtained with Matlab, the post-processing software chosen in this experiment.

Before going right into the measurement results and observations, some acronyms used have to be clarified. The tags 'OR', 'XOR', 'SC' and 'EGC' refer to the Ordinary Wave, the Extraordinary Wave, the Selection Combining and the Equal-Gain Combining, respectively.

4.1 Early results

Earlier studies in an nearly-identical link were performed during the 2018 / 2019 academic year[7]. It is interesting to know some information about this first experiment, as it was performed by the same author and the same research team.

The old experiment involved a link using the same nodes and antenna infrastructure. The antennas were tuned to the 5.24MHz frequency (frequency chosen based on the solar variation and its actual cycle), this being 160kHz lower than the one used in this experiment. This section is interesting as it affected the design of the experiment presented in this document. The band used in the link in the previous study (5.24MHz) presented loads of interferences in the link and made it impossible to study correctly all the advantages of polarization diversity in NVIS technologies. With this known and revising the Observatori de l'Ebre diagrams [28], the 5.4MHz frequency was chosen.

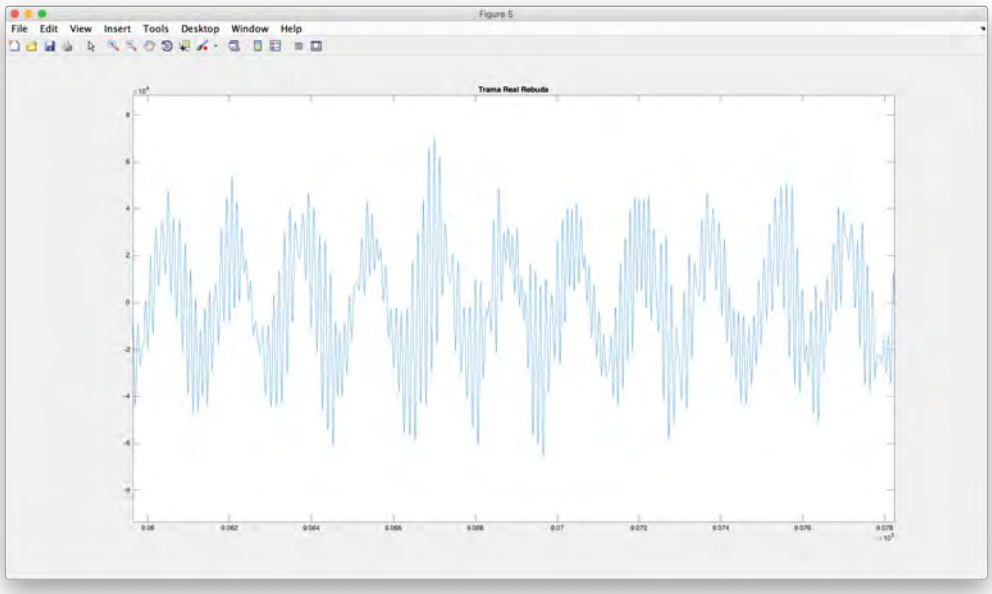

Figure 4.1: Interferences in the 5.24MHz band near Cambrils[7]

Another important result to take into account is related to the power study realized in this project. As the tests were performed doing a power sweep between 3W and 100W, different conclusions are obtained, as explained afterwards in this document. All the results with the 100W transmitting power have been dismissed as they were too good due to the high transmission strength. As this link is meant to be implemented with a sensor network or similar, the 100W is not an ideal frequency and the results are not applicable to the real world.

4.2 EbNo Graphs

E_b/N_0 CDF According to Polarization Techniques

E_b/N_0 appears as a way to measure the power received per each bit. An interesting first study is the analysis of the E_b/N_0 received from the ordinary wave, the extraordinary waves and the E_b/N_0 post-processed by the application of polarization techniques. Obviously, all these four values will be compared in order to complete the research. Firstly, it is also interesting to define what exactly E_b/N_0 reffers to. The E_b/N_0 of the signal frame received

is calculated as:

$$\frac{Eb}{No}(dB) = SNR(dB) + 10log10(B) - 10log10(R_b) \tag{4.1}$$

In equation 4.1, the Rb acronym is the bitrate of the signal (parameter that depends on the modulation order test), B is the noise bandwidth where we take measure of the BER (in our case is the data bandwidth, 2.3 kHz) and the SNR is the Signal Noise Ratio of the signal.

A really fascinating graph to generate in the telecommunications environment is the CDF graph of one of the variables under study. The cumulative distribution function (CDF) of a parameter evaluates its probability that this parameter will take a value less than or equal to a desired amount. The first graphs of this document will be the CDF E_b/N_0 of the received signals and its different diversity combining techniques and polarizations.

In Figure 4.2 we can see the first result of this study. A CDF is displayed, where the probability to receive a given E_b/N_0 value is shown, depending on four different factors. Therefore, four lines are exhibited, representing the Ordinary Wave received, the Extraordinary wave received, or the combination of these two waves with diversity combining techniques; applying Selection Combining or Equal-Gain Combining. The plot shows its legend for a better comprehension.

The Y-axis in Figure 4.2 displays the probability P($E_b/N_0 <$ Xo) of receiving an E_b/N_0 less or equal than the value Xo shown on the X-axis. The graphic has been obtained with the combination of the received signals at transmitting power of 50W, and using only the 4QAM modulation.

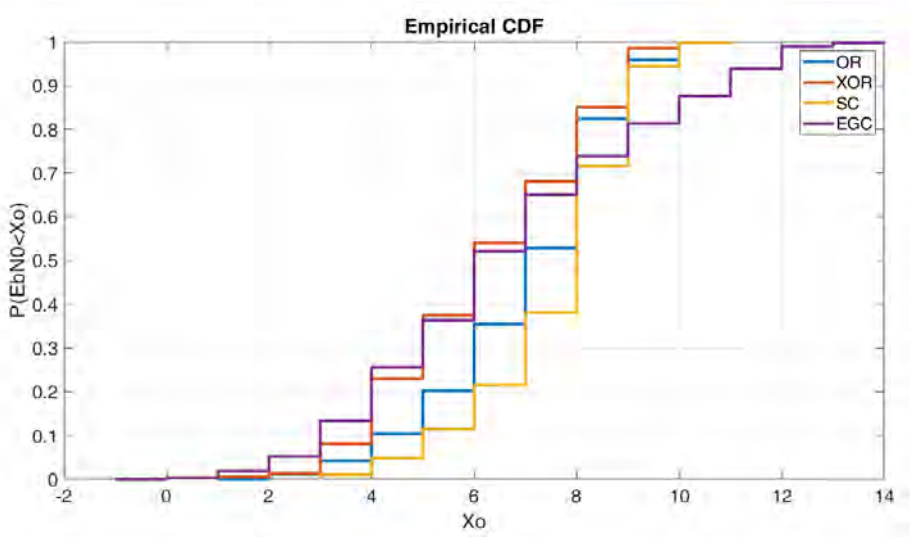

Figure 4.2: E_b/N_0 CDF of 4QAM at 50 W[3]

If we analyse the graph in Figure 4.2, it can be clearly seen that if our signal is received by the ordinary and extraordinary waves, there is a little more probability to receive a higher E_b/N_0 by the ordinary layer. This result is quite logical as the ordinary wave in the ionosphere is present more hours a day than the extraordinary one. Taking a look and comparing the diversity combining techniques when using polarization diversity, the Selection Combining (SC) technique seems to be the best option in order to receive always the highest E_b/N_0 of the ordinary and the extraordinary layer, and to maximize the robustness of the system. If we study the worst case scenario while using the Equal-Gain Combining (EGC) technique, the E_b/N_0 results obtained can match the lower E_b/N_0 of the ordinary or extraordinary layers. This affirmation depends completely on the electromagnetic noise that is added to our signal while travelling through the ionosphere. On the other hand, and studying the best case scenario, and comparing it with the usage of the Selection Combining method, up to extra 3dBs can be obtained with a probability of 1%. Despite this low percentage, the graph also shows that the Equal Gain Combining technique has a 20% probability to obtain a higher E_b/N_0 than the Selection Combining technology. Furthermore, there is a 35% of chances to obtain the same E_b/N_0 results than when the Selection Combining. These results has been obtained by analysing closely Figure 4.2. To sum up,we can conclude that the Equal Gain Combining method performs better with higher E_b/N_0 values, and than the Selection Combining is the best performer when using lower E_b/N_0 values.

These first results are logical as we are studying and comparing a order 4 modulation while using a high transmitting power of 50W. Using lower transmission powers will lower the performance of the link, specially when the Equal Gain Combining method is analysed. This is because, with lower transmission power, the chances of adding noise to our signal are

greater.

E_b/N_0 versus Time According to Polarization Techniques

As explained in earlier chapters in this document, the ionosphere's behaviour changes throughout the day. Studying how this affects the scenario is an interesting result of the research done. This section will focus on the comparison of the ionospheric characteristic waves separately during the day, together with the comparison of the Selection Combining and Equal Gain Combining techniques all over the day's hours.

The mean E_b/N_0 value received during different hours of the day is shown in Figure 4.3. The results have been obtained using a 4QAM modulation and a transmission power of 50 W. As it can be seen, the E_b/N_0 received by the ordinary and extraordinary waves differs on a maximum of 3 dB, confirming a decorrelation between the channels. As this graph has been generated with the mean values per hour, higher decorrelation values could be obtained by studying each frame and packet separately, obtaining a graph similar to Figure 2.7. This specific and more precise study will be left for future lines of the project.

Analysing the diversity combining techniques, it can be stated that the Selection Combining's E_b/N_0 is always higher than the E_b/N_0 received by the singular ordinary or extraordinary waves. This result is completely consistent as the Selection is based on the signal's Signal to Noise Ratio, and selects the signal with the highest SNR value. A rare result also appears in the graph under study, Figure 4.3. At 11 UTC (X-axis) the mean value of the selection Combining is below the E_b/N_0 value received by the Extraordinary wave. Studying deeply the graph, approximately in 65% of the day's hours the E_b/N_0 received using the Equal-Gain Combining technique is higher that the one received in the ionospheric waves alone. Comparing the two diversity combining techniques, it can be affirmed that the Selection Combining method receives higher E_b/N_0 than the Equal-Gain Combining method in approximately 90% of the day's hours. To conclude, and studying only the ionosphere's characteristic waves, the graph shows that the ordinary and extraordinary waves can have an E_b/N_0 difference up to 3dB.

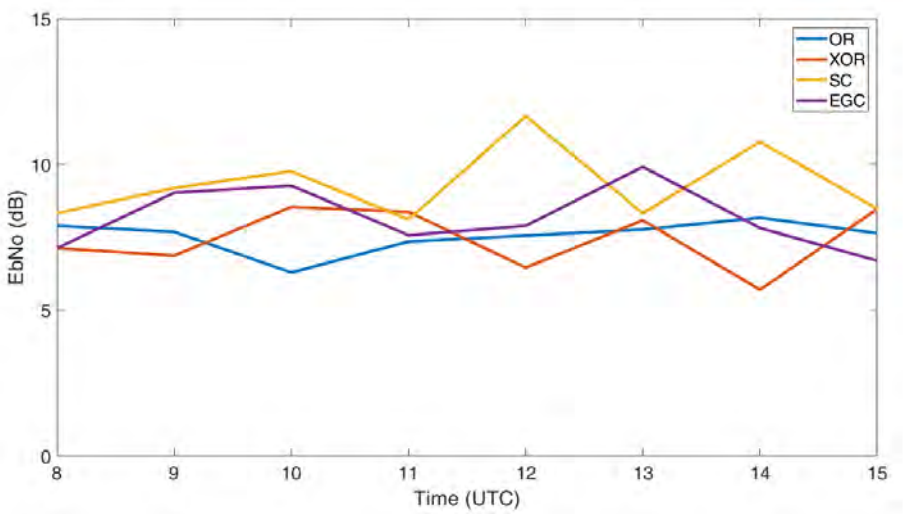

Figure 4.3: E_b/N_0 vs Time for 4QAM at 50 W[3]

Taking a look to the Figure 4.3 X-axis, it can be observed that only 7 hours appear out of the 24 hours that a day has. This is because the results out of the graph's hours aren't the desired and the ones under study as this project is focused in a single frequency. For a full-day coverage, multiple frequencies should be used. Chapter 5 in this document gives a deeper study on the channel's availability and a better understanding of the figure above.

4.3 BER graphs

BER CDF According to Polarization Techniques

Studying the power of the signals received is indispensable when studying a telecommunications link. Nevertheless, this aspect has to be complemented with other parameters in order to achieve a complete link study. A fundamental parameter to study is the Bit Error Rate (BER), which measures the number of incorrect bits received compared to the total number of bits transmitted. This first BER study will be realized comparing different order and modulations transmitted and received by the ionosphere's characteristic waves and polarization diversity techniques.

Order 4 modulations will be the first ones to be analysed and studied. Firstly, figure 4.4 shows that the behaviour of the 4PSK and 4QAM modulations have nearly-identical results when received using singular ionospheric waves and no diversity techniques applied. In both ordinary and extraordinary waves and both modulations, a 80% probability to receive a BER lower than 10^{-4} is presented. On the other hand, the 4FSK modulation has 57% of proba-

bility to receive a BER lower than 10^{-4}, being clearly the worse out of the three modulations.

Analysing the diversity combining techniques, the Selection method seems to be the best choice for all three modulations. Specifically, there are very high chances to achieve a BER lower than 10^{-4}: the 4PSK achieves it with a probability of 96%, the 4FSK with a probability of 88% and the 4QAM with a probability of 85%. A good performance is also perceived when using the Equal-Gain Combining method achieving BERs lower than 10^{-4} with a probability of 82% with the 4PSK and 4QAM modulations and 59% with the 4FSK modulation.

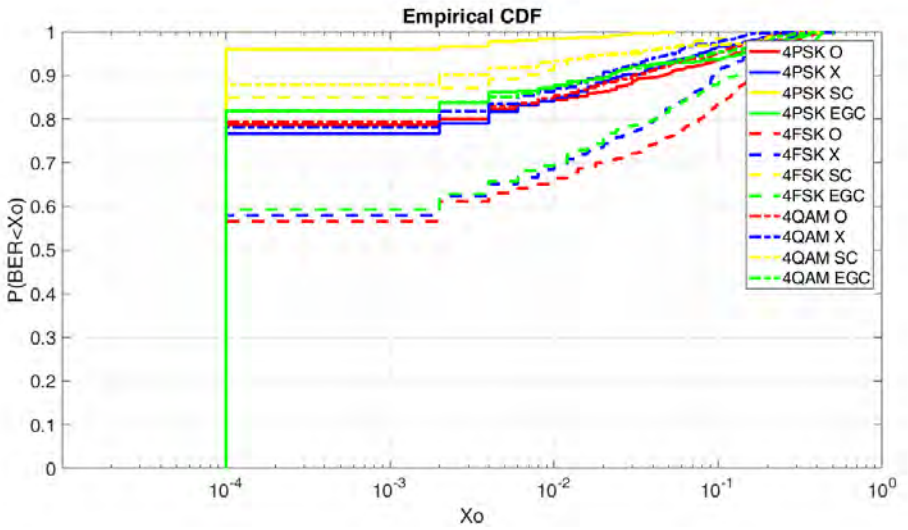

Figure 4.4: Bit Error Rate (BER) CDF of order 4 modulations at 50W.[3]

If a more complex modulation order is analysed, a decrease in the probabilities to achieve low BERs can be appreciated due to the reduction of the E_b/N_0 received. After studying the order 4 results, the two following graphs will study the order 8 and order 16 measurements. Order 32 results have been dismissed due to the low E_b/N_0 received.

Figure 4.5 shows the results for order 8 modulations. Taking a look at the two ionospheric characteristic waves individually, there is approximately a probability between 42% and 55% for the 8PSK to achieve a BER lower than 10^{-4}, a probability between 8% and 26% for the 8FSK to accomplish the same result, and a probability between 1% and 24% for the 8QAM to reach the same BER value (10^{-4}). Therefore, the 8PSK presents the better results than the other two modulations, on account of the constellation distribution.

Studying the different combining techniques, Selection Combining is still the best option for both the 8PSK and 8FSK with, respectively, 70% and 40% to attain a BER lower than 10^{-4}. If we study the 8QAM Selective Combing and Equal-Gain Combining methods, both have got the same results in this scenario, with a 39% of probability to achieve a BER lower

than 10^{-4}. This result is nearly identical for the Equal-Gain Combining using the 8FSK modulation. As a last result, the 8PSK modulation when using Equal Gain Combining has a probability of 50% s to achieve a BER lower than 10^{-4}. To sum up, the best modulation is again the PSK, and the best results are again attained while using the Selection Combining method.

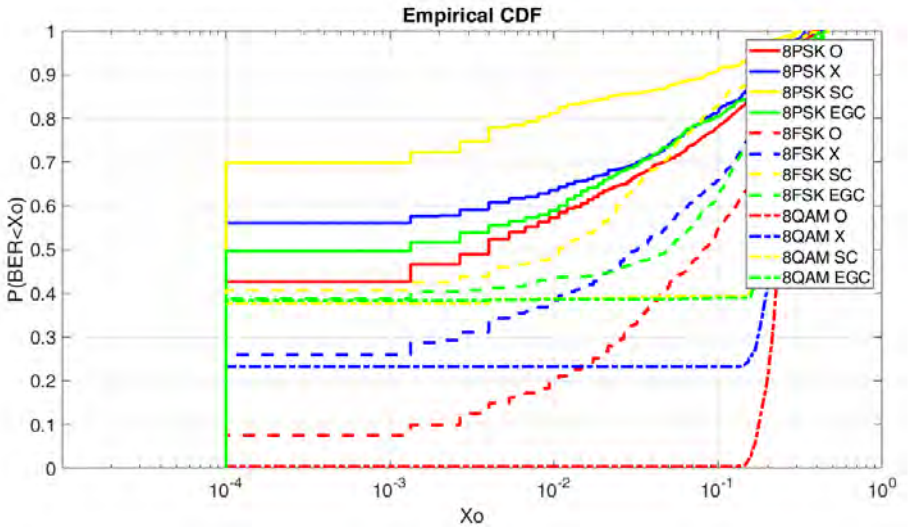

Figure 4.5: Bit Error Rate (BER) CDF of order 8 modulations at 50W.[3]

The results for the 8PSK applying Selection Combining are remarkably good. Despite that, if the modulation order is increased to 16, the transmitting power of 50W isn't enough to achieve the E_b/N_0 enough to attain a good BER result.

Figure 4.6 shows the order 16 results for the tests performed. Studying the 16QAM and 16FSK modulations, there is a probability of 1% to accomplish a BER lower than 10^{-2}. Similar as the results before, the PSK is still the best modulation to use in the NVIS link developed. The 16PSK obtains the same results as the other modulations with about 17% of probability, and can aim to obtain even a BER of 10^{-4} with a probability between 6% and 8%.

The results obtained when using diversity technique are notably good. When using Selection Combining and a 16PSK modulation, a BER lower than 10^{-4} is received with a 25% or probability (approximately 4 times the results without applying diversity techniques). When using the Equal-Gain Combining method the probability to attain the same result becomes a 21%, also a great result compared to the ionosphere's waves individually. Furthermore, the other two modulations (16QAM and 16FSK) also obtain a great improvement by the use of the Selection Combining and the Equal-Gain Combining. The results are almost the same for both polarization techniques, with near a 20% of probability to obtain a BER lower than 10^{-4}.

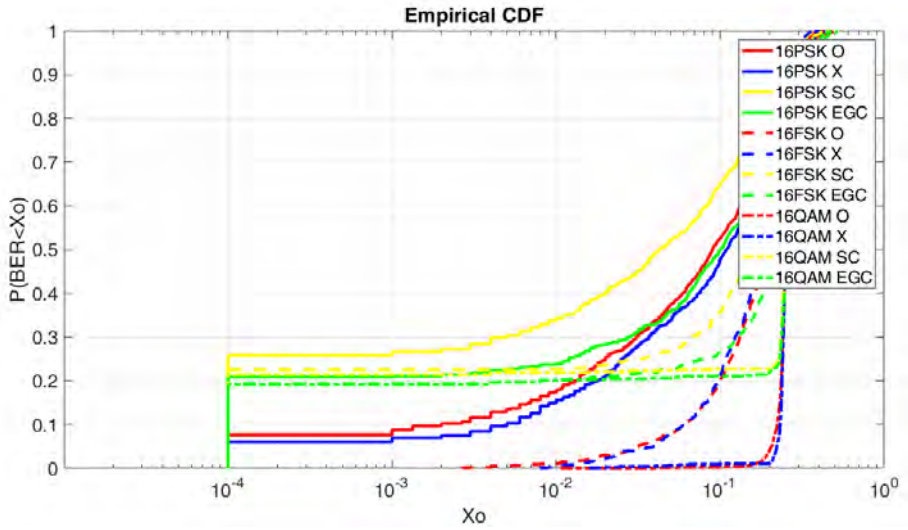

Figure 4.6: Bit Error Rate (BER) CDF of order 16 modulations at 50W.[3]

BER CDF According to Power Transmission

As the previous results have shown, the power transmission of 50W is not enough to provide good results when using high-order modulations, which are an objective in order to increase throughput and data rates. The order 16 modulations and their results denote a high decrease of the probabilities to achieve low BERs, which is one of the main goals of this link's evaluation.

Despite the results obtained in Figure 4.6, it has been proven that the Selective Combining brings the best results when working together with the PSK modulation. Nevertheless, 50W is a rather high transmitting power for the NVIS applications, which are mainly remote sensing and simple-infrastructure areas. To give a better idea on how the scenario performs, a power sweep between 6 and 50W using the modulation orders 4 and 8 is given below. Based on the results above, only the best combination of diversity technique and modulation will be studied, these being the PSK modulation and the Selection Combining technique.

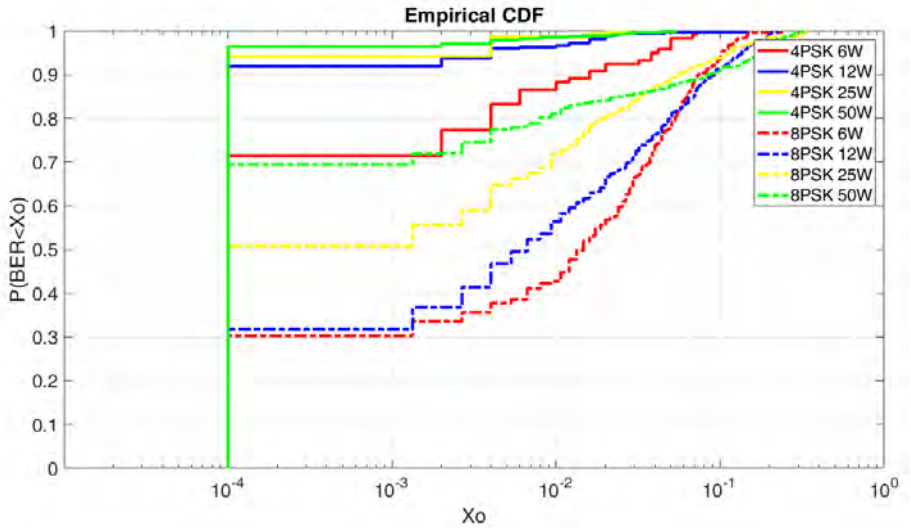

Figure 4.7: SC BER CDF according to power transmission[3]

As can be seen in Figure 4.7, the 4PSK attains the best results regardless of the power of transmission. Even tho the 8PSK results are worse, more bitrate can be reached when using the higher-order modulation. If the graph is analysed, the 4PSK modulation has a 96%, 94%, 92% and 71% of probabilities to achieve a BER lower than 10^{-4} whit a power transmission of 50W, 25W, 12W and 6W, respectively. On the other hand, the 8PSK with transmitting powers of 50W, 25W, 12 W and 6 W has a 69%, 50%, 32% and 30% of probabilities to achieve a BER lower than 10^{-4}.

4.4 Number of Transmissions According to Selection Combining

To have a better understanding on the performance of the scenario, and after studying different parameters and measurements of our link, another graph has been generated. This last graph has the goal to take extra conclusions about which is the best order modulation and power transmission to use when working with Selection Combining in our research. A Bernoulli distribution will be analysed, focusing on the probability to receive a BER lower than 10^{-4} after several retransmissions.

The results are displayed in Figure 4.8. The graph proves that when using a 4PSK modulation with a transmitting power of 12W, 25W and 50W there is a total of 99% of probabilities to achieve a BER lower than 10^{-4} if the packet is retransmitted. When using the same modulation with a lower transmitting power (6W) or when using a 8PSK modulation with a high transmitting power (50W) the results are identical, attaining a BER lower than

10^{-4} with a probability of 99% with 4 transmissions. In order to have more examples, with two transmissions the probability to reach a BER lower than 10^{-4} is 91%, and with three transmissions the probabilities to attain the same BER is 97%.

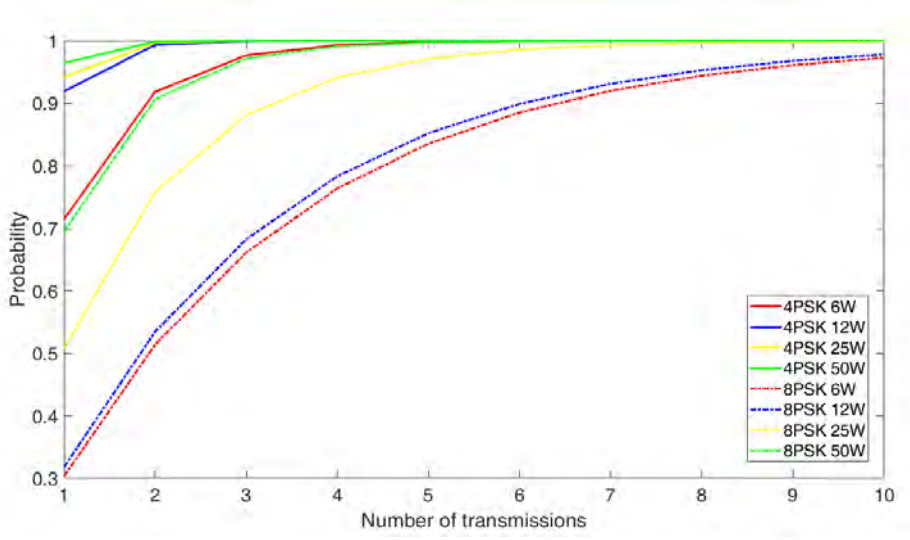

Figure 4.8: Number of transmissions according to Selection Combining[3]

Some early observations can be obtained with this graph. The PSK modulation with an order equal to 4 is a great choice in our link. One transmission using 50W, 12W or 12W has great outcome. On the other hand, using a lower transmission power is not a bad choice either, as if we re-transmit the same signal we have a great chance (more than 90%) to achieve a BER lower than 10^{-4}. This solution can be useful in low-power oriented systems with low consumption. On the other hand, if the order 8 of the modulation is chosen (8PSK), higher transmission powers are needed but higher throughput is obtained.

Chapter 5

Channel Study

The ionosphere and its electromagnetic properties act to generate two separate channels when a signal of a certain frequency reaches this region of the atmosphere. The study of these two channels, the one generated by the ordinary wave and the one generated by the extraordinary wave, is interesting in order to fully understand the behaviour of the ionosphere. This study is essential to be able to apply different telecommunications techniques to improve the performance of NVIS links.

Three different channel parameters have been studied in this project, leaving further research for future lines and continuations of this investigation. The three aspects studied are the Doppler Shift, the Doppler Spread and the Channel's Availability throughout the day.

5.1 Doppler Shift

Figure 5.1 analyzes the Doppler shift produced by the clocks of the Red Pitaya platform used in the scenario implemented. The Doppler shift in our case is directly related to the temperature of the platform, which will affect the stability of the clock, as explained in earlier chapters in this document. The Doppler shift caused by the ionosphere is completely negligible compared to the variation of the clocks due the implementation of our technology in a low cost platform. As the link implemented and its nodes used are rather cheap, low stability clocks are normal. A good frame design and a good post-processing of the signals received is then key to mitigate the negative effects of the usage of low-cost technologies and to reach the goal of the development a consistent but cheap node network.

Figure 5.1 exhibits a boxplot for all the hours of the day when the channel is active. A boxplot is a special representation of a variable and is interpreted like this: the red line is the mean Doppler Shift received, the blue square the 50% of the Doppler Shift received, the black line is the 25% upper and down Doppler Shift received and the red crosses are outliers

(data point that differs significantly from other observations [33]).

It can be appreciated that the maximum doppler shift received is -19.5Hz and the maximum -15Hz, a much higher value than the ionosphereric layer's doppler shift. This doppler shift calculated has been computed and compensated with the Matlab software thanks to the 600Hz tone added to the frame.

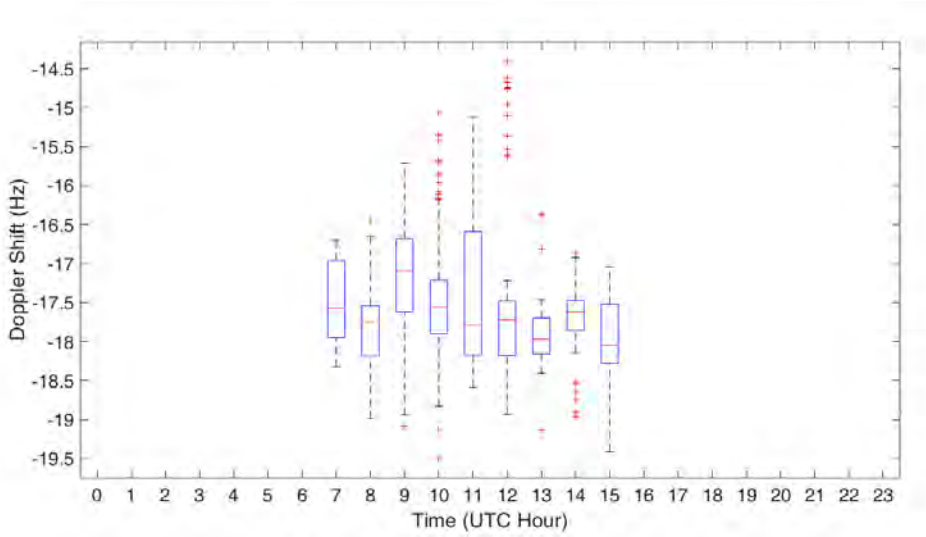

Figure 5.1: NVIS Total Doppler Shift vs Time

5.2 Doppler Spread

The Doppler spread is an important parameter to study of any telecommunication channel, and gives information about the variability of the channel (Chapter 2 gives a further explanation of this concept). As in the previous case, the information is shown in a graph with the value of the doppler spread throughout the day.

Figure 5.2 and Figure 5.3 exhibit the Doppler Spread of the Ordinary wave's Channel and the ExtraOrdinary wave's channel, respectively. The boxplot is interpreted as follows: the red line is the mean Doppler spread received, the blue square the 50% of the Doppler spread received, the black line is the 25% upper and lower Doppler spread received, and the red crosses are outliers.

As it can be appreciated, he maximum Doppler spread of the ordinary channel is about 0.038 Hz and the minimum near 0.02 Hz. This value is a key issue to determine the maximum time of the data block, as this values are directly related to the coherence time of the channel.

On the other hand, the extraordinary channel's values are approximately 0.055 Hz as a maximum and 0.023 Hz as a minimum. Similar results by both channels are obtained.

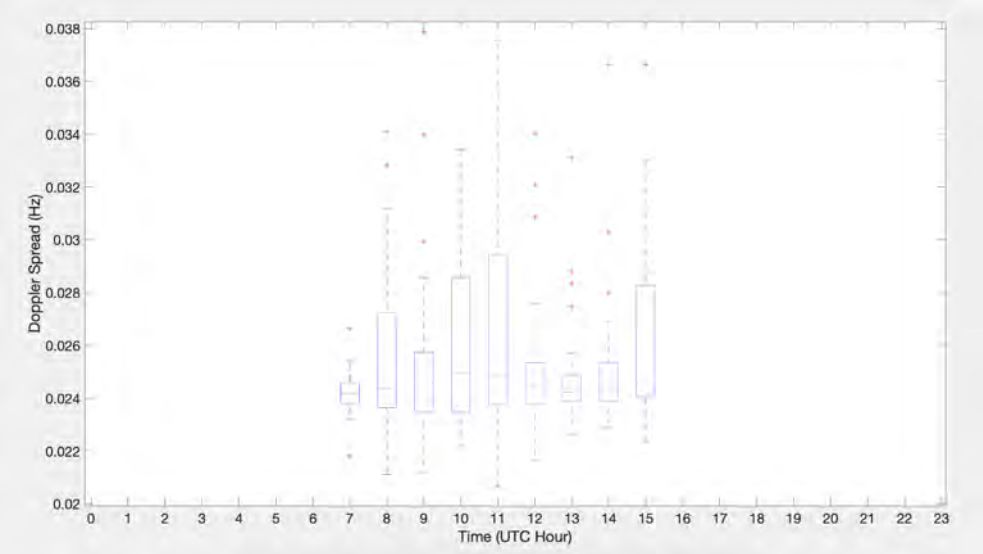

Figure 5.2: NVIS Total Doppler Spread vs Time of the Ordinary Channel

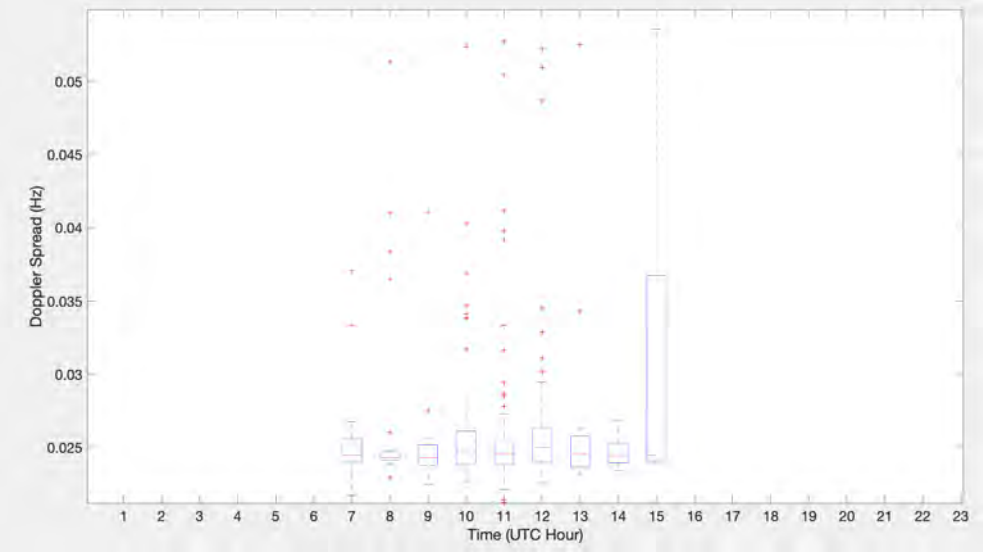

Figure 5.3: NVIS Total Doppler Spread vs Time of the ExtraOrdinary Channel

Despite the results obtained, there are a great amount of outliers in the boxplots above. To give more perspective about the maximum and minimum doppler spread results, Figure 5.4 and Figure 5.5 show the actual highest and lowest values of the parameter under study.

For the ordinary channel, the maximum value received has been 2 Hz and the minimum around 0.02 Hz. For the other channel under study, the results are similar, and also peak around 2 Hz and have a valley with a value near 0.02 Hz.

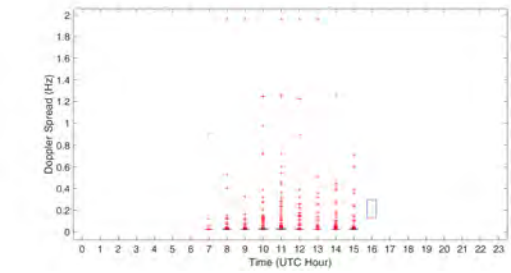

Figure 5.4: NVIS Total Doppler Spread vs Time of the Ordinary Channel

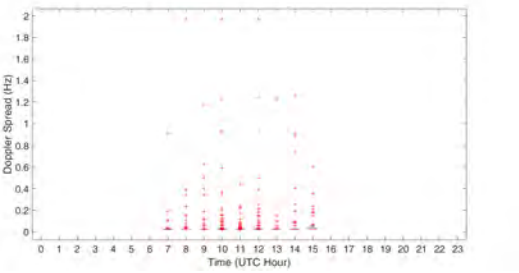

Figure 5.5: NVIS Total Doppler Spread vs Time of the ExtraOrdinary Channel

5.3 Channel Availability

The last study performed in this research is the evaluation of the availability of the implemented link between Barcelona and Cambrils. Figure 5.4 display the percentage of packets detected and demodulated at 5.4 MHz in the reception point in Cambrils. It is key to analyze this graph to understand the impact of the received frames in other graphics based on the time, like others in previous chapters. The availability has been defined as follows: the highest number of packets demodulated in a certain hour has been computed. This number has been defined as the peak performance (corresponding to the 100% in our graph). The number of packets demodulated in the remaining hours has been escalated based on this factor and then displayed in the graph.

Studying Figure 5.4, it can be seen that the channel is not active up until 6 UTC time (8 a.m. time in the Catalonia region) and stops being active at 16 UTC time (6 p.m. in the Catalonia region). This result is logic as the sunrise and the sunset in the month when the tests were performed (December) corresponds approximately to the hours of the activation and deactivation of the ionospheric channels. On the other hand, both channels remain active during a total of 10 hours, having the best availability between 7 UTC and 14 UTC (9 a.m. and 4 p.m. in Catalonia). This high availability corresponds to the day's most solar activity.

If we compare both channels, we can say that the performance given by both is similar. The ordinary channel is a bit better as it reaches a peak of more packets demodulated, and does not lower the yield up until the sunset, with some individual valleys throughout the

day. The extraordinary channel has a similar behaviour, lowering its performance on the sunset and having also some valleys during daytime. An interesting point of the graph is the decorrelation that both channels suffer, confirming that the appliance of polarization diversity techniques is a complete success for links that can benefit from this channels differences.

Another observation that can be extracted from Figure 5.4 is the relationship between a frequency and its availability coverage. If a single frequency can cover with good results approximately 8 or 9 hours of a day, a total of three different frequencies could give a perfect availability to the link. Furthermore, these three frequencies would be simple to implement and develop (or even add to our existing system), as a simple antenna with different traps could fulfil the requirements, without the need of a multiband antenna.

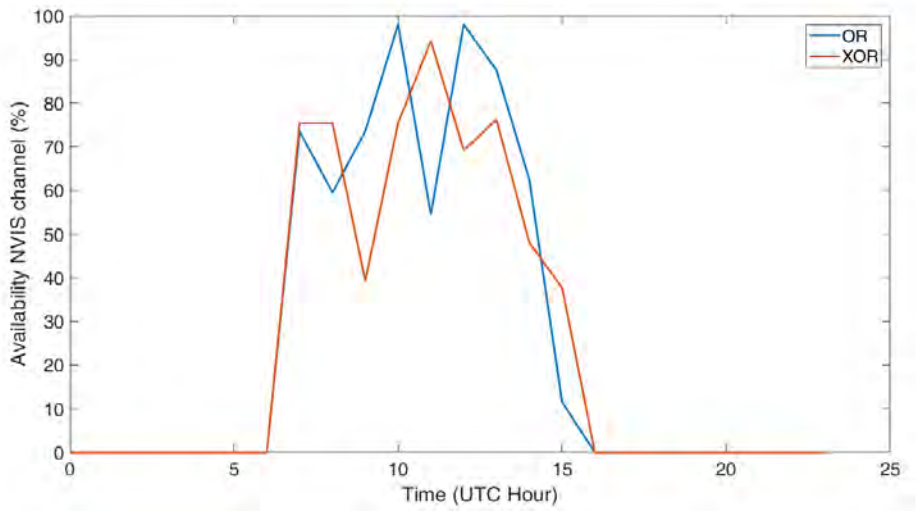

Figure 5.6: Availability of the Barcelona - Cambrils NVIS Ionospheric channels

Chapter 6

Conclusions

After a first project to develop an NVIS SIMO link between Barcelona and Cambrils [7], this project had the main objective of the deep study of different modulations, transmitting power and diversity technique for a link based in the one developed previously. Different conclusions can be extracted from all the results displayed in this document.

Firstly, and after analyzing the results obtained, it can be observed that the ordinary and extraordinary waves are not received with the same E_b/N_0, as they can differ up to 3dB. These power differences and decorrelations between the two channels provide the possibility to apply polarization diversity techniques to take advantage of this fact.

Using the polarization diversity with different diversity combining techniques have also resulted in important findings. It can be concluded that the Selective Combining technique is the combining method that maximizes the received E_b/N_0 while using both ordinary and extraordinary waves. As a consequence to this, this combining technique also implies the reception of lower BER results. Analysing the other combining technique used, Equal-Gain Combining, the results are also remarkable. This second method can obtain an E_b/N_0 up to 3dB above than the highest E_b/N_0 received by the ordinary and extraordinary waves. Nevertheless, this possibility depends completely on the received electromagnetic noise, and is limited to 1% of probability as graphs above show. On the other hand, it has been also proven that this technique is 20% more probable to receive a higher E_b/N_0 than the highest received by the ordinary and extraordinary waves.

The PSK, FSK and QAM modulations of orders between 2 and 32 with different power transmissions have also been studied and compared, analysing all of them for four different channels: the Ordinary Wave's channel, the Extraordinary Wave's channel, and the different combining techniques with the appliance of polarization diversity. It can be concluded that, regardless the usage of the diversity, the BER obtained for modulations of order 16 or higher is not low enough to assure a communication when using a transmitting power of 50W. The usage of 100W has been discarded due to the application of this study, which can mainly

be related to sensors and low-cost platforms. Furthermore, the results have proven that the usage of PSK modulations with polarization diversity and Selection Combining presents the best results in both BER and E_b/N_0. Specifically, 4PSK and 8PSK modulations with Selection Combining and power transmissions between 6 W to 50 W present the better results. Three combinations of power and modulation can be highlighted out of all the tests performed. The 4PSK modulation with powers of 6W and 12 and the 8PSK with a power of 50W are the clear successors of the research performed.

To summarize the comparisons just realized, table 6.1 exhibits all the information explained above.

Power consumption	**Diversity Combining Technique**	**Modulation**	**Bitrate**	**Probability to obtain BER** 10^{-4}
6W	SC	4PSK	2.9Kbps	71%
12W	SC	4PSK	2.9Kbps	92%
50W	SC	8PSK	5.8Kbps	70%

Table 6.1: Application summary

The three featured setups have different purposes. For instance, if our remote sensing system requires a low power usage, the option that uses a 4PSK with a power transmission of 6 W is the better option. In this case we would have a probability of a 71% to receive a BER lower than 10^{-4}, and 99% of probability to have the same BER if we make two retransmissions (worst case scenario). On the other hand, if our remote sensing system can make use of high power transmissions, the best option will be the usage of the 8PSK modulation with a transmission power of 50 W. This option would double the bitrate of the 4PSK option, and would have a 70% of probability to receive a BER lower than 10^{-4} (with a 99% of probability if two retransmissions are performed, worst case scenario). Finally, if our remote sensing network requires both low power consumption and needs the reception of all the packets without retransmissions, the best option would be the 4PSK modulation with a power transmission of 12 W. In this case, we would have a 92% of probability to receive a BER lower than 10^{-4}, up to a 99% of probability if we make only one retransmission. In addition, the designed scenario can be further improved. The application of an Error Correction Code (ECC) would highly increase the probabilities of receiving correctly the first packet transmitted as it help noisy channels as the one used in this research.

The usage of diversity techniques can also open new horizons for remote sensing. The robustness provided by these technologies can compensate the lower gains of compact antennas, making them more usable on HF communications or allowing low power transmissions for remote sensing. This second application is remarkable, as it would decrease the battery

consumption and would make the usage of renewable energies more viable.

To end, some conclusions can also be extracted from the channel study realized. First of all, the study of the Doppler Shift has proven that a low cost platform has some inconveniences (higher doppler shift due to the Red Pitaya clocks than the ionosphere's doppler shift). A well-designed frame working together with a powerful post-processing of the signal are key to mitigate the channel's negative effect (up to ±20 Hz in our infrastructure case).

The study of the doppler spread also has some highlights to be mentioned. The ordinary and extraordinary channels have some differences on the mean doppler spread value received, resulting in two completely different channels as they present different performances on this channel parameter. Despite that, both channels peak (around 2 Hz) and bottom (around 0.02 Hz) almost identically, fact that allow us to use the same coherence time for both channels.

Lastly, the channel's availability has demonstrated that one frequency can have a good yield during approximately 9 hours of the day (37.5% of daytime). The usage of three different frequencies would mean a complete coverage and a full availability of the channel, and it would also be easy to implement with, for instance, antenna traps. Another conclusion from the availability study is the confirmation of the decorrelation between both channels throughout the day.

6.1 Future Research

The next step to be taken to continue the work done in this project is associated with the channel study. The research done in this document corresponds to a single-frequency channel study, being this frequency 5.4 MHz. A complete wide-band channel study from 3 MHz to 10 MHz would be key in order to improve the channel's availability throughout the day, and to complete the comparison of the ordinary and the extraordinary channels.

Another step to be taken is directly related to the infrastructure used. This project presents a complete study with one antenna in transmission and two in reception (SIMO). The following pass would be the implementation of a MIMO 2x2 link, which would open the possibility of adding capacity to our actual system. Furthermore, space-time block codes (Alamouti's code, for example) could be applied in transmission, enabling the transmission multiple copies of a data stream across a number of antennas to improve the reliability of data transfer.

Figure 6.1 gives a graphical idea of the study of the possible evolution from SIMO to MIMO. The application of space-time codes is shown, together with the usage of polarization diversity (two different channels are shown). A setup like the presented below would

definitely contribute in the improvement of the NVIS technology.

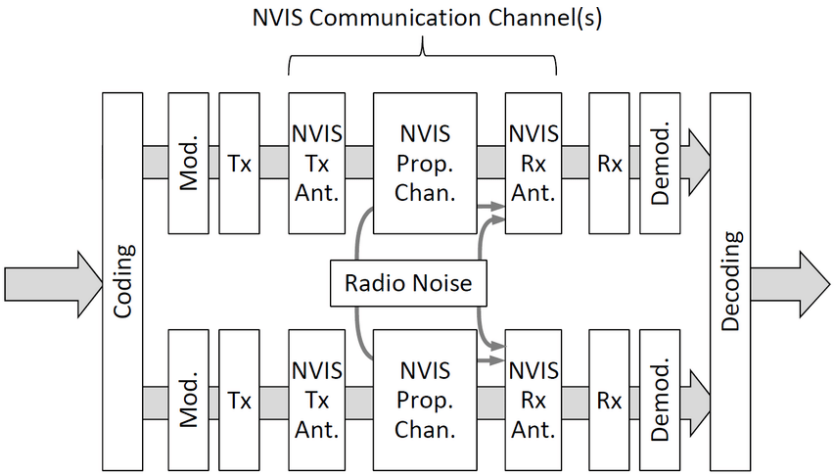

Figure 6.1: Block diagram of an NVIS communication system. Two propagation channels are shown, as in diversity and Multiple Input, Multiple Output (MIMO) systems. [8]

The usage of more complex modulations and transmission multiplexations is another important pass in order to complete the scenario developed. Using multiple carriers with, for example, an OFDM (Orthogonal Frequency Division Multiplexing) multiplexing might be an option to improve the link. Other more complex modulations could be applied the this multiplexing and new horizons could be opened depending on the results obtained. A lot of current technologies use this OFDM modulations, being 4G and 5G the main character and the most known.

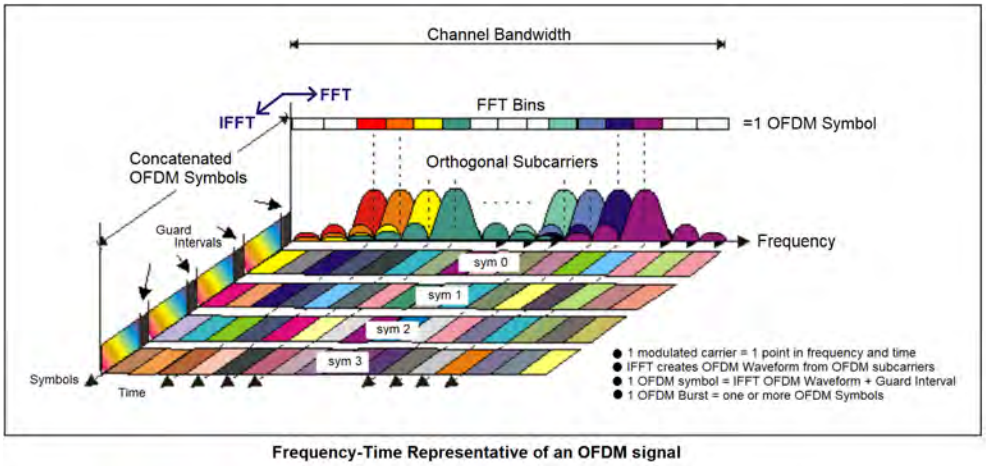

Figure 6.2: Combined time/frequency domain view of OFDM signal [34]

Annex A

Ionospheric Polarization Techniques for Robust NVIS Remote Sensing Platform

The author of this document and his team developed and published an article regarding the results obtained. MDPI's Applied Sciences journal published the article on the 28th of May of 2020. The whole paper is attached below.

applied sciences

MDPI

Article

Ionospheric Polarization Techniques for Robust NVIS Remote Sensing Platforms

Josep M. Maso, Jordi Male, Joaquim Porte, Joan L. Pijoan * and David Badia

La Salle Campus, Ramon Llull University, 08022 Barcelona, Spain; josep.maso@salle.url.edu (J.M.M.); jordi.male@salle.url.edu (J.M.); joaquim.porte@salle.url.edu (J.P.); david.badia@salle.url.edu (D.B.)

* Correspondence: joanlluis.pijoan@salle.url.edu

Received: 27 April 2020; Accepted: 26 May 2020; Published: 28 May 2020

check for updates

Featured Application: Less power consumption, robust, and faster near vertical incidence skywave remote sensing platforms.

Abstract: Every year more interest is focused on high frequencies (HF) communications for remote sensing platforms due to their capacity to establish links of more than 250 km without a line of sight and due to them being a low-cost alternative to satellite communications. In this article, we study the ionospheric ordinary and extraordinary waves to improve the applications of near vertical incidence skywave (NVIS) on a single input multiple output (SIMO) configuration. To obtain the results, we established a link of 95 km to test the diversity combining of ordinary and extraordinary waves by using selection combining (SC) and equal-gain combining (EGC) on a remote sensing platform. The testbench is based on digital modulation transmissions with power transmission between 3 and 100 W. The results show us the main energy per bit to noise spectral density ratio (E_b/N_0) and the bit error rate (BER) differences between ordinary and extraordinary waves, SC, and EGC. To conclude, diversity techniques show us a decrease of the power transmission need, allowing for the use of compact antennas and increasing battery autonomy. Furthermore, we present three different improvement options for NVIS SIMO remote sensing platforms depending on the requirements of bitrate, power consumption, and efficiency of communication.

Keywords: HF; NVIS; SIMO; diversity combining; remote sensing platform

1. Introduction

The world's communications have gone from the communication between millions and millions of people to billions and billions of "things." The current networks are focused in urban areas with many devices (NB-IoT, Lora-Wan, Sigfox [1,2]) and people (3G, 4G, GSM). Although these networks are remarkably large, they experience difficulties in remote areas. The main obstacle for the development of these networks in isolated zones is the difficulty of reaching the installation terrain, often due to the complicated orography. In such situations, the only viable solution is satellite communication, which leads to a high-cost and complex infrastructure, making the transceiver unfeasible to be integrated with a remote sensing platform.

Although the satellite alternative seems notably solid, regions like the North and South Poles do not present coverage, thus making it difficult to get data from remote sensors. Some works [3–9] in high frequency (HF) communications validate the viability of ionospheric communications in remote areas [10]. This alternative proposes a new network for remote Internet of Things (RIoT) scenarios. Combining the ionosphere as a channel with HF (frequencies from 3 to 10 MHz) creates the near vertical incidence skywave (NVIS) channel. The proposed link makes a coverage of up to 250 km without the need of a line of sight when using an incidence angle from 70° to 90°. All these aspects are

essential to develop a network with a low economic cost and a straightforward installation, resulting in an interesting alternative to satellite communications.

Although there are some previous works related to the performance of this channel [3–9], this study shows how some physical characteristics of the ionosphere will improve the performance of the NVIS channel.

The ionosphere is defined by having different layers. When using it as a channel, the link is mainly established with the F2 layer and, during maximum solar incidence, with the E layer. As the ionization of the atmosphere is directly affected by the Sun, the star's variation makes the NVIS channel very unstable, leading to undesired fading, interferences, and link losses. This ionization also affects the refraction index, creating two characteristic waves, the ordinary and the extraordinary. Reflected waves present different polarizations, which can be used for applying diversity techniques to improve robustness and capacity.

The study of geoscience, when applied to engineering systems, allows us to develop a new telecommunications platform for remote areas and remote sensing applications. Analyzing the performance of the ionosphere as a telecommunication channel will contribute to upgrading the yield of this network for remote communications. This work proves that the understanding and use of the ordinary and extraordinary waves [11] from the F2 layer of the ionosphere [12] lead to an improvement in the NVIS channel's performance. Moreover, applying single input multiple output (SIMO) [13] techniques to circular polarized antennas [14] will allow the system to receive both characteristic waves simultaneously, thus further increasing the channel's yield.

Ben A. Witvliet in [15] and Yvon Erhel in [13] measured the correlation between the ordinary and extraordinary waves; the results stated an isolation of at least 13 dB. Our work not only studies the behavior of the characteristic waves but also demonstrates that this channel de-correlation can lead to an improvement in the ionospheric link.

U. Umaisaroh in [16] studied the NVIS channel with a 2×2 MIMO link. An improvement of the communication's capacity is achieved, as it focused on the throughput improvement compared to a SISO environment. In contrast to this, our work focuses on the economic cost of the overall system and the transmitting power, which are aspects not studied in [13].

Reference [13] also showed how the capacity of the ionospheric channel is improved by using both waves, but all the tests were realized with a 500 W power amplifier. Although it proves that using both waves improves the performance of the channel, is not tested in a data transmission protocol for a low power consumption platform.

Finally, our work proposes a comparison with different diversity combining algorithms (selection combining and equal-gain combining), merging both waves to improve the performance and the robustness of the NVIS channel.

This article is organized as follows. In Section 2, we explain the bases of the NVIS ordinary and extraordinary waves and their use on polarization techniques. In Section 3, we describe the developed system used to perform the tests. In Section 4, we detail the frame design and the tests performed. In Section 5, we present the results obtained of the tests. Finally, Section 6 contains the conclusions achieved.

2. NVIS Characteristics

In this section we explain in more detail the principal characteristics of the NVIS propagation, especially those of the ordinary and extraordinary waves. Moreover, we explain the use of these ionospheric waves to perform polarization diversity and diversity combining.

2.1. Ordinary and Extraordinary Waves

NVIS communications are completely dependent on the ionosphere and its behavior to the Sun. As the ionization of the upper layers of the ionosphere is strongly dependent on the Sun's radiation, the ionosphere varies both daily and seasonally.

Because the energy from the Sun varies both daily and seasonally, the ionosphere is never static. The Sun, for instance, has times of extreme activity that causes storms and severe disruption to the propagation. Moreover, the ionosphere's behavior is affected by even more parameters, such as the height and the mixture of gasses [17].

This chemistry that was just mentioned also directly affects the rate of ionization, just as the density of atoms and the intensity of radiation do. Some chemical reactions take place quickly, causing high ionization, while others are slower, resulting in less ionization [10].

All the ionization that was explained illustrates the ionosphere's interaction with radio waves. When a radio wave reaches the ionosphere, the electric field in the wave forces the electrons in the ionosphere into oscillation at the same frequency as the radio wave. Some of the radiofrequency energy is released due to this resonant oscillation, on which the oscillating electrons may either re-combine, thereby losing the radio energy, or re-radiate the original wave energy (refraction) [17].

The refraction phenomenon is fundamental in all ionospheric links, and it occurs because ionized molecules present free electrons that are able to vibrate in response to the radio signals reaching them. The behavior of each of these moving electrons resembles small dipole antennas. Radio waves are bent away from areas of high ionization because these areas have a lower refractive index. This bending effect reduces as the radio wave frequency increases, until a point where it suddenly stops, letting the waves pass on through (this value is known as the critical frequency) [17].

As a result to the electron's vibration, it is quite normal for a radio wave to have its polarization changed by the ionosphere. Furthermore, waves of different polarization can be refracted in different amounts. This leads to their return to Earth in two different rays: the ordinary and extraordinary rays, both with distinct properties [10]. Just as with reflections from other layers of the atmosphere or at other times, these rays can have different phases, amplitudes, frequencies, and times of arrival [17]. These different properties can be used in order to improve telecommunication links, as polarization diversity techniques are an option in ionospheric channels.

2.2. *Polarization Diversity and Diversity Combining*

Polarization diversity was firstly applied to HF, radar, and imaging systems. Its potential for improving the capacity of wireless communications systems was demonstrated, despite some disappointing premature predictions [18]. The improvement generated by this diversity method is typically granted by an additional de-correlated channel provided by a polarization state that is orthogonal to the existing one.

NVIS communications can clearly benefit from polarization diversity techniques due to one of these aspects: the two characteristic wave components with circular polarization of the opposite sense, both of which follow a different path through the ionosphere when a radio wave of a certain frequency reaches the ionosphere. The other key issue with evaluating parameters in this kind of scenario is cross-polarization discrimination (XPD), with low correlation co-efficients being achieved in most situations. Nevertheless, considerably more attention has been paid to spatial diversity due to the significant difference in the mean received signal level between the co-polarized and cross-polarized branches when one polarization is transmitted. Yet, spatial diversity is not the best solution after all, since at least 20λ horizontal and 15λ vertical separation distances are required for efficient outdoor diversity, resulting in an attraction gain for polarization diversity [19].

The implementation of a diversity system based on polarization needs some extra infrastructure compared to a rather simple scenario. As with any other diversity environments, multiple antennas are needed, specifically at the receiver. Both multiple input multiple output (MIMO) and SIMO are valid solutions, with the MIMO being the one that provides a better performance as it involves multiple antennas in the transmitter.

The effectiveness and success of both HF MIMO systems and diversity reception increases with the decrease of the correlation between the received signals. If the de-coupling between both characteristic waves is large enough and our system is correctly designed to combine the diversity

correctly, these features will drastically improve HF MIMO and diversity reception. In [18], the behavior and the correlation of the two ionospheric characteristic waves were studied, where both signals achieved de-correlations that can reach values like 13 dB easily. Taking into account the propagation mechanism studied and the clear isolation (more than 12 dB) between both characteristic waves, it is safe to state that a scenario that implements diversity reception can greatly benefit from the use of a pair of orthogonal circularly polarized antennas. Specifically, the use of right-hand circular polarization (RHCP) and left-hand circular polarization (LHCP) antennas for HF MIMO will create two very isolated channels that will maximize MIMO gain. In the study done in this article, though, the transmit antenna will be a linear polarized one while having two circular polarized antennas in the receiver.

All diversity techniques need a process for combining the different signals that arrive at the receiver. There are a lot of them, each one presenting different characteristics and gains. This article studies two different techniques: the selection combining, a method that selects the strongest signal received and discards the other, and the equal-gain combining, a technique that sums all the signals received coherently.

3. System Description

The main challenge of the performed tests is to analyze the influence of the ordinary and extraordinary ionospheric waves at the same time through an NVIS channel. Furthermore, the system requires us to analyze at the same time both ionospheric waves and apply polarization techniques to reach the best results on the demodulation of the frame. To achieve the goal, it is necessary to have a reconfigurable software defined radio platform.

One of the main disadvantages in the design of the transmission platform for an ionospheric link is having the ability to mitigate the effects of the channel. Due to new digital technologies, these processes are becoming more efficient and less costly. In addition, one of the main challenges is to develop a flexible platform that allows for the development of all the tests to be validated and for the implementation of all the tests and study hypotheses. All these requirements are solved with field-programmable gate array (FPGA) platforms.

To do this and to develop a low-cost platform, we have chosen the STEMlab 125-14 board hardware from the manufacturer Red Pitaya [20]. The main core of this hardware is a Zynq-7010-SOC [21]. These products contain a one-core (or two cores depending on which product is chosen) ARM® Cortex™-A9 [22] based processing system (PS), plus 28 nm of Xilinx programmable logic (PL). In addition, this board has different peripherals (see in Figure 1) that allow us to make a robust platform for remote sensing:

- Zynq (FPGA/Cortex): The FPGA is essentially dedicated to data processing and the Cortex to time and data management. In the reception, this module allows us to receive and process the received signals in the analog digital converters (ADCs). This data is sent in real time to the Cortex via direct memory access (DMA). The Cortex is dedicated to saving the information on an external hard disk. In transmission, the Cortex contains the information that will be sent to the FPGA to be transmitted.
- Converters: The board has two channels, with two analog digital converters (ADCs), with a resolution of 14 bits and a sampling frequency of 125 MSPS. These, along with the two SMA connectors, will allow us to receive the signal by the antenna, send it to the FPGA, and treat the signal. The two ADCs allow us to receive both ordinary and extraordinary waves at the same time. This synchronization allows us to make a fair comparison with all the different polarization techniques. As opposed to ADC converters, digital analog converters (DACs) have a single converter to manage the two converter channels from the digital to the analog world; this fact should be considered when implementing the transmitter of the system. These will allow us to take out the signal already treated by the antenna. Therefore, this peripheral is only used by the FPGA [23].

- RaspBerry PI-3 [24]: This second post-processor is added to help the main core to control peripherals and save the received frames. The connection between both boards is realized via Ethernet.
- Amplifier: To carry out the various soundings with the FSK, QAM, and PSK modulations and with the transmissions of non-constant envelope modulations (QAM), using a class A amplifier is necessary. To carry out the study, an amplifier with a maximum power of 250 W was installed [25], although the maximum testbench power transmission is about 100 W and the minimum 3 W.
- Filters: The platform contains two band-pass filters (BPF). The first transmitter is a band HF band-pass filter from 3 to 10 MHz. This frequency range is defined for the NVIS channel. The second one, is defined from 4 to 6 MHz to filter possible interferences.
- GPS: The synchronization in time between the transmitter and the receiver is accomplished via GPS.
- Post-processing data: Finally, the post-processing of the data is performed by MATLAB software [26]. This is used to demodulate all the tests frames received and to obtain the results' graphics.

Appl. Sci. **2020**, *10*, x FOR PEER REVIEW 5 of 16

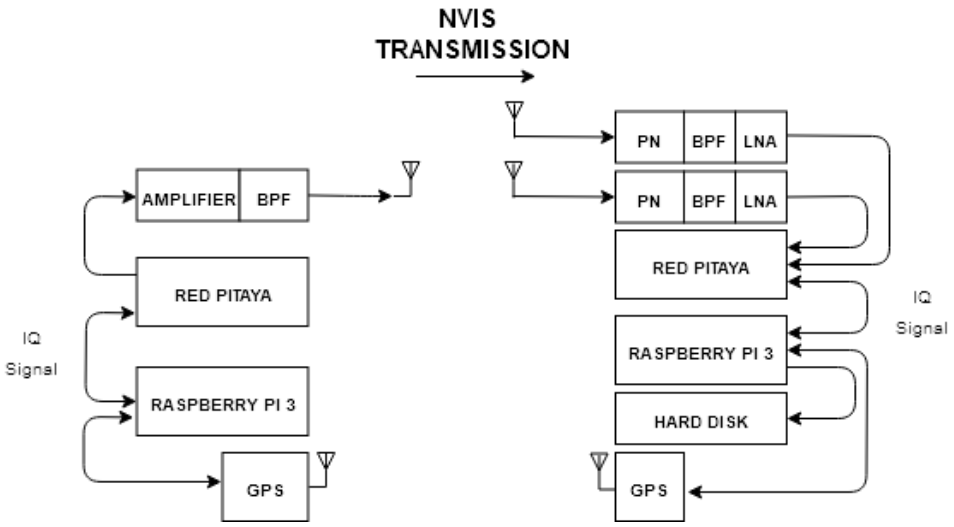

Figure 1. Schematic of the remote sensing platform.

Figure 1. Schematic of the remote sensing platform.

The three antennas of the experiment are completely identical. All three are made of a flat copper conductor in the shape of inverted Vee and are tuned to the frequency of 5.40 MHz. The choice of the antenna design (inverted Vee) is based on its building facilities—they are easy to build as they only need a mast—and based on its gain, as it is similar to the horizontal dipole. Moreover, they are ideal for NVIS as they have a good radiation pattern in the upward direction.

The frequency was chosen and calculated from the revised ionograms of Observatori del Ebre [27]; this frequency is lower than the cutoff frequency as it allows us to correctly receive ordinary and extraordinary waves from the ionosphere. Concretely, and because of the study of the ionogram, it was possible to determine that the ideal frequency for the transmission to make the wave rebound with the minimum of possible losses is 10% less than the critical frequency F2.

The transmitter is less complex than the receiver as it only has one antenna. The reception part of the scenario is more sophisticated, as our experiment follows a single input multiple output design. The two reception antennas are set perpendicularly. This configuration together with a phasing network that delays one antenna from the other will allow the system to receive different polarizations at the same time, which is the main goal of the scenario itself.

A phasing box was designed and implemented to realize the delays mentioned with coaxial delay lines. The box gets a total of four wires, two from each antenna, we get two identical signals for each antenna with a radio frequency splitter. The paths of the two antennas are the same, as follows: one feed line is connected directly to a RF combiner, and the one cable is lengthened with a quarter wave phasing line to provide a 90° phase shift. The output of the box gives us a phase difference between the dipoles antennas of either +90° and −90°. For the designed system, the phasing network

The three antennas of the experiment are completely identical. All three are made of a flat copper conductor in the shape of inverted Vee and are tuned to the frequency of 5.40 MHz. The choice of the antenna design (inverted Vee) is based on its building facilities—they are easy to build as they only need a mast—and based on its gain, as it is similar to the horizontal dipole. Moreover, they are ideal for NVIS as they have a good radiation pattern in the upward direction.

The frequency was chosen and calculated from the revised ionograms of Observatori del Ebre [27]; this frequency is lower than the cutoff frequency as it allows us to correctly receive ordinary and extraordinary waves from the ionosphere. Concretely, and because of the study of the ionogram, it was possible to determine that the ideal frequency for the transmission to make the wave rebound with the minimum of possible losses is 10% less than the critical frequency F2.

The transmitter is less complex than the receiver as it only has one antenna. The reception part of the scenario is more sophisticated, as our experiment follows a single input multiple output design. The two reception antennas are set perpendicularly. This configuration together with a phasing network that delays one antenna from the other will allow the system to receive different polarizations at the same time, which is the main goal of the scenario itself.

A phasing box was designed and implemented to realize the delays mentioned with coaxial delay lines. The box gets a total of four wires, two from each antenna, we get two identical signals for each antenna with a radio frequency splitter. The paths of the two antennas are the same, as follows: one feed line is connected directly to a RF combiner, and the one cable is lengthened with a quarter

wave phasing line to provide a 90° phase shift. The output of the box gives us a phase difference between the dipoles antennas of either +90° and −90°. For the designed system, the phasing network is for one single frequency. For a multiple frequency receptor, the phasing network should be done in digital. Figure 2 shows a diagram of the phasing network designed.

Appl. Sci. **2020**, *10*, x FOR PEER REVIEW 6 of 16

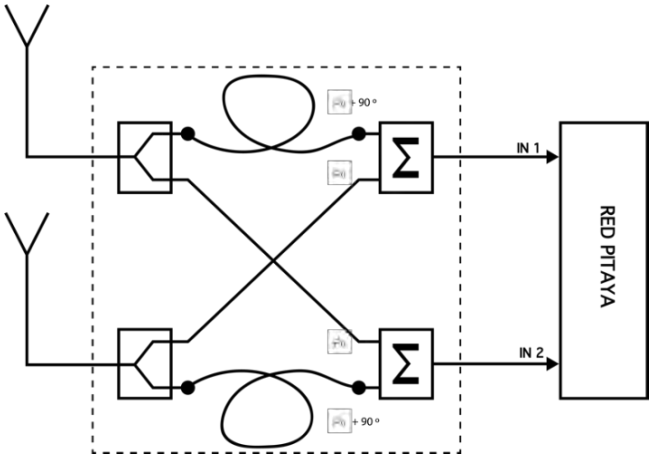

Figure 2. Diagram of the phasing network.

Figure 2. Diagram of the phasing network.

The goal of the phasing network is to unify the two antennas (initially linearly polarized and orthogonal to each other) so that two circularly polarized antennas are created. Specifically, the polarization vectors of the antennas are the following:

$$LHCP_{Antenna} = \hat{x} + j \cdot \hat{y}, \quad (1)$$

$$RHCP_{Antenna} = j \cdot \hat{x} + \hat{y}, \quad (2)$$

The goal of the phasing network is to unify the two antennas (initially linearly polarized and orthogonal to each other) so that two circularly polarized antennas are created. Specifically, the polarization vectors of the antennas are the following:

$$LHCP_{Antenna} = \hat{x} + j \cdot \hat{y}, \quad (1)$$

$$RHCP_{Antenna} = j \cdot \hat{x} + \hat{y}, \quad (2)$$

Equation (1) belongs to left-hand circular polarization, which corresponds to the ordinary wave in the Northern Hemisphere. Equation (2), the extraordinary wave, was studied, and it demonstrated that it has the lesser delay and RHCP in the Northern Hemisphere, while the ordinary wave has the greater delay and LHCP [18].

Equation (1) belongs to left-hand circular polarization, which corresponds to the ordinary wave in the Northern Hemisphere. Equation (2), the extraordinary wave, was studied, and it demonstrated that it has the lesser delay and RHCP in the Northern Hemisphere, while the ordinary wave has the greater delay and LHCP [18].

4. Tests Performed

In this section we show the scenario where we take the tests and the frame design of the signals transmitted.

4.1. Test Scenario

The performance tests were carried out in the Catalonia region (Spain), where we established a link between two NVIS nodes. The transmitter node was located at La Salle University-URL in Barcelona, and the receiver node was located at a remote location in Cambrils (Tarragona). In Figure 3, we can see the receiver node with two perpendicular inverted Vee antennas. The link between both locations is about 96 km, ensuring an NVIS communication as we can see in Figure 4. The receiver was not set in Barcelona due to the high electromagnetic noise and interference at the HF band. For that reason, it was preferable to set the receiver in Cambrils. The tests performed were taken for 15 days from 7 December to 22 December 2019. The frames were transmitted every minute during these days.

4. Tests Performed

In this section we show the scenario where we take the tests and the frame design of the signals transmitted.

4.1. Test Scenario

The performance tests were carried out in the Catalonia region (Spain), where we established a link between two NVIS nodes. The transmitter node was located at La Salle University-URL in Barcelona, and the receiver node was located at a remote location in Cambrils (Tarragona). In Figure 3, we can see the receiver node with two perpendicular inverted Vee antennas. The link between both locations is about 96 km, ensuring an NVIS communication as we can see in Figure 4. The receiver was not set in Barcelona due to the high electromagnetic noise and interference at the HF band. For that reason, it was preferable to set the receiver in Cambrils. The tests performed were taken for 15 days from 7 December to 22 December 2019. The frames were transmitted every minute during these days.

Figure 3. Receiver node in Cambrils (Spain).
Figure 3. Receiver node in Cambrils (Spain).
Figure 3. Receiver node in Cambrils (Spain).

Figure 4. Near vertical incidence skywave (NVIS) test link.
Figure 4. Near vertical incidence skywave (NVIS) test link.

4.2. Frame Design
4.2. Frame Design
4.2. Frame Design

To achieve the expected results in the tests, one of the most important parts of the study is the design of the frame to be transmitted. Every test consists of the transmission of the frame design in Figure 5. The signal frame is composed of a total amount of 50 packets, and every packet is principally formed by three different modulations (PSK, FSK, and QAM). To synchronize the system with every modulation and to correct all the channel effects, every modulation is preceded by a 600 Hz tone and a PN sequence. In Figure 5, we can see that every data block contains 250 symbols with a resample of 42, resulting in a 2.3 kHz bandwidth. Another important detail about the frame design is the time of each packet, which was carefully chosen to fulfill the coherence time requirements of the ionosphere [28]. Taking into account the most restrictive coherence time as 1.46 s [11], we set the time of each packet at 510.36 ms. To compare the effects of the ordinary and extraordinary waves to the modulation on the frame at 510.36 ms. To combine the effects of the ordinary and extraordinary waves to the transmitted, it is important to transmit every packet in the coherence time. The total duration of the 50 packets is about 25 s.

Once the system identifies the start of the frame, the first block is the 600 Hz tone. This tone of a duration of 60 ms is a key issue for correcting the Doppler shift, which affects the rest of the block. The Red Pitaya platform clocks have a low stability, which creates a Doppler shift effect higher than the
To achieve the expected results in the tests, one of the most important parts of the study is the design of the frame to be transmitted. Every test consists of the transmission of the frame design in Figure 5. The signal frame is composed of a total amount of 50 packets, and every packet is principally formed by three different modulations (PSK, FSK, and QAM). To synchronize the system with every modulation and to correct all the channel effects, every modulation is preceded by a 600 Hz tone and a PN sequence. In Figure 5, we can see that every data block contains 250 symbols with a resample of 42, resulting in a 2.3 kHz bandwidth. Another important detail about the frame design is the time of each packet, which was carefully chosen to fulfill the coherence time requirements of the ionosphere [28]. Taking into account the most restrictive coherence time as 1.46 s [11], we set the time of each packet at 510.36 ms. To compare the effects of the ordinary and extraordinary waves to the modulation on the frame at 510.36 ms. To combine the effects of the ordinary and extraordinary waves to the transmitted, it is important to transmit every packet in the coherence time. The total duration of the 50 packets is about 25 s.

Once the system identifies the start of the frame, the first block is the 600 Hz tone. This tone of a duration of 60 ms is a key issue for correcting the Doppler shift, which affects the rest of the block. The Red Pitaya platform clocks have a low stability, which creates a Doppler shift effect higher than the
The Red Pitaya platform clocks have a low stability, which creates a Doppler shift effect higher than

the ionosphere. Our measurements of the platform show us that the maximum value of the Doppler shift received due to the low stability clocks is about ±20 Hz. The 600 Hz tone lets us identify the Doppler shift inserted by its variations between 580 and 620 Hz. In the worst case, if we consider a received tone frequency of 580 Hz, the measurement could be done with 34 cycles (60 ms). If we make use of a DC constant instead of a 600 Hz tone, the measurement will be done with the 16th part of a cycle (60 ms), which is not enough to take a real measurement.

The second block present on the frame is a 6th order PN sequence. The PN sequence is used for synchronizing with the modulations. The resampling of the PN sequence is about 8 and has a total duration of 5.12 ms. The order and duration of the PN sequence were carefully designed to avoid the channel effects of a delay spread, Doppler spread, and Doppler shift.

Finally, the data blocks allow us to study the robustness of each modulation with different polarization techniques. The study performed was done with three different modulations (PSK, FSK, and QAM) with variating orders between 2 and 32 for power transmissions between 3 and 100 W.

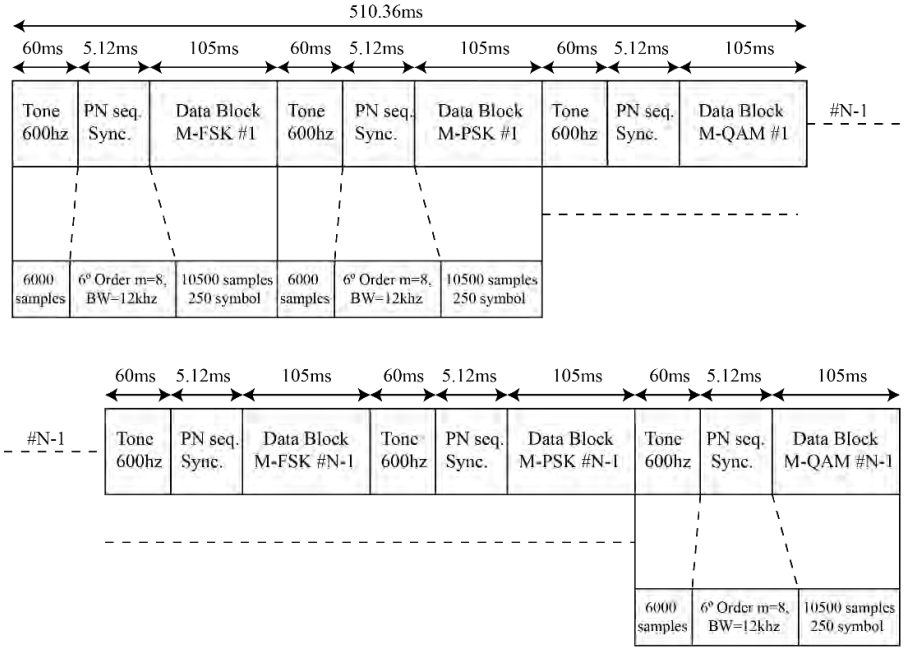

Figure 5. Frame design.

Figure 5. Frame design.

4.3. Testbench

4.3. Testbench

The entire set of tests was classified by order modulations between 2 and 32 and power transmissions between 3 and 100 W. For all of them, the bandwidth was set to 2.3 kHz, and we made use of three modulations (PSK, FSK, and QAM). After this, we obtain the results depending on the ionospheric layer reflected and depending on the polarization technique used by MATLAB post-processing. In one hour we perform 25 tests, as we can see in Table 1.

Table 1. Testbench transmitted.

Order of Modulation	Power Transmission	Minute
2, 4, 8, 16, 32	3 W	05, 06, 07, 08, 09
2, 4, 8, 16, 32	6 W	15, 16, 17, 18, 19
2, 4, 8, 16, 32	12 W	25, 26, 27, 28, 29
2, 4, 8, 16, 32	25 W	35, 36, 37, 38, 39
2, 4, 8, 16, 32	50 W	45, 46, 47, 48, 49
2, 4, 8, 16, 32	100 W	55, 56, 57, 58, 59

Table 1. Testbench transmitted.

Order of Modulation	Power Transmission	Minute
2, 4, 8, 16, 32	3 W	05, 06, 07, 08, 09
2, 4, 8, 16, 32	6 W	15, 16, 17, 18, 19
2, 4, 8, 16, 32	12 W	25, 26, 27, 28, 29
2, 4, 8, 16, 32	25 W	35, 36, 37, 38, 39
2, 4, 8, 16, 32	50 W	45, 46, 47, 48, 49
2, 4, 8, 16, 32	100 W	55, 56, 57, 58, 59

power spectral density (E_b/N_0) and the effectiveness of the application of polarization techniques to obtain the best demodulation results. The tags "OR," "XOR," "SC," and "EGC" indicate the ordinary wave, the extraordinary wave, the selection combining, and the equal-gain combining, respectively.

5. Results

In this section we analyze the most relevant results obtained from the tests performed. We will see the influence of the ordinary and extraordinary waves on the modulation's bit energy to noise power spectral density (E_b/N_0) and the effectiveness of the application of polarization techniques to obtain the best demodulation results. The tags "OR," "XOR," "SC," and "EGC" indicate the ordinary wave, the extraordinary wave, the selection combining, and the equal-gain combining, respectively.

5.1. E_b/N_0 CDF According to Polarization Techniques

First of all, we measured the relationship between the E_b/N_0 received from the ordinary and extraordinary waves and the E_b/N_0 post-processed by the application of polarization techniques. The E_b/N_0 of the signal frame received is calculated as:

$$\frac{Eb}{N0}(dB) = \mathrm{SNR(dB)} + 10 \cdot \log 10(B) - 10 \cdot log10(Rb), \quad (3)$$

where the Rb is the bitrate of the signal (depending on the modulation order test), B is the noise bandwidth where we take the measurement of the bit error rate (BER) (which in our case is 2.3 kHz), and SNR is the signal noise ratio of the signal.

To analyze the relationship, we make use of the cumulative distribution function (CDF). In Figure 6, we can see the CDF where it represents the probability to receive a given E_b/N_0 value depending on whether it is received by the ordinary or extraordinary waves or by the application of a polarization technique. The *y*-axis shows us the probability $P(E_b/N_0 < Xo)$ of receiving an E_b/N_0 less than or equal to value Xo of the *x*-axis. The graphic is obtained with the received signal of all power transmissions, which in this case is of a 4QAM.

First of all, we can see in Figure 6 that if we receive our signal by the ordinary and extraordinary waves, we have a slightly higher probability to receive a higher E_b/N_0 by the ordinary layer. In the case of using a polarization technique, the selection combining technique looks to be the best option to always receive the highest E_b/N_0 of the ordinary and the extraordinary layers. In the worst case, with the equal-gain technique, depending on the electromagnetic noise, we can obtain the same E_b/N_0 as the lower E_b/N_0 of the ordinary or extraordinary layer. In contraposition, in the best case, we can obtain 3 dB more than the selection combining technique in a probability of 1%. Despite this low probability, we have a 20% probability to obtain a higher E_b/N_0 than selection combining, as we can see in Figure 6. Furthermore, we have a 35% probability to obtain the same results as selection combining.

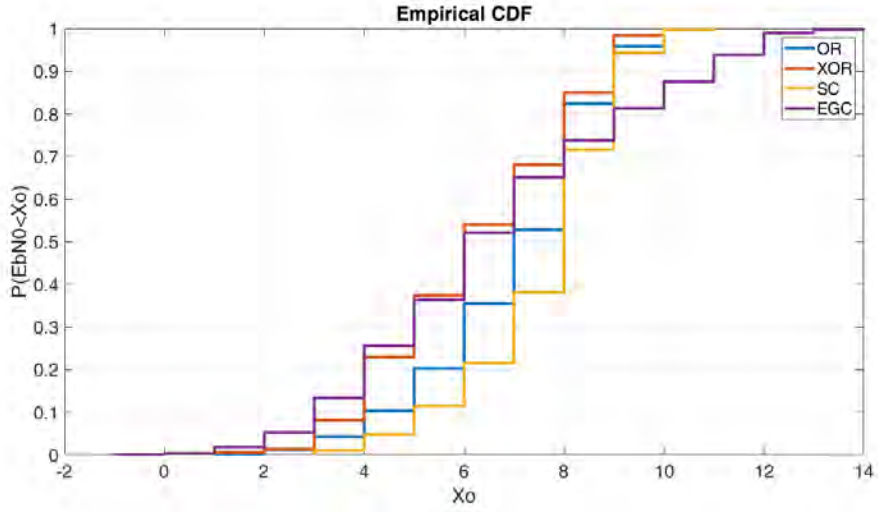

Figure 6. Bit energy to noise spectral density (E_b/N_0) cumulative distribution function (CDF) of 4QAM at 50 W.

Figure 6. Bit energy to noise spectral density (E_b/N_0) cumulative distribution function (CDF) of 4QAM at 50 W.

First of all, we can see in Figure 6 that if we receive our signal by the ordinary and extraordinary waves, we have a slightly higher probability to receive a higher E_b/N_0 by the ordinary layer. In the case of using a polarization technique, the selection combining technique looks to be the best option to always receive the highest E_b/N_0 of the ordinary and the extraordinary layers. In the worst case, with the equal-gain technique, depending on the electromagnetic noise, we can obtain the same E_b/N_0 as the lower E_b/N_0 of the ordinary or extraordinary layer. In contraposition, in the best case, we can obtain 3 dB more than the selection combining technique in a probability of 1%. Despite this low probability,

we have a 20% probability to obtain a higher E_b/N_0 than selection combining, as we can see in Figure 6. Furthermore, we have a 35% probability to obtain the same results as selection combining.

5.2. E_b/N_0 versus Time According to Polarization Techniques

5.2. E_b/N_0 versus Time According to Polarization Techniques

From another point of view, we can analyze the behavior of the ionospheric waves and the polarization techniques by the mean E_b/N_0 received during different hours of the day. In Figure 7, we can observe the results obtained by a 4QAM transmitted at 50 W. As we can see, the E_b/N_0 received by the ordinary and extraordinary waves differs by a maximum of 3 dB. We can analyze that mainly the selection combining E_b/N_0 is always higher than the E_b/N_0 received by the ordinary and extraordinary waves. Rarely, as we can see at 11 UTC, the mean of the selection combining is under one of the E_b/N_0 received by the ionospheric layer. On the other hand, for 50% of the hours, by equal-gain combining, we received a higher E_b/N_0 than the ionospheric waves, and for 12% of the hours, a higher E_b/N_0 was received than by selection combining. For the other 50% of the hours, we received E_b/N_0 between the received E_b/N_0 of the ordinary and extraordinary waves. On the other hand, we can analyze that the ordinary and extraordinary waves can have an E_b/N_0 difference up to 3 dB.

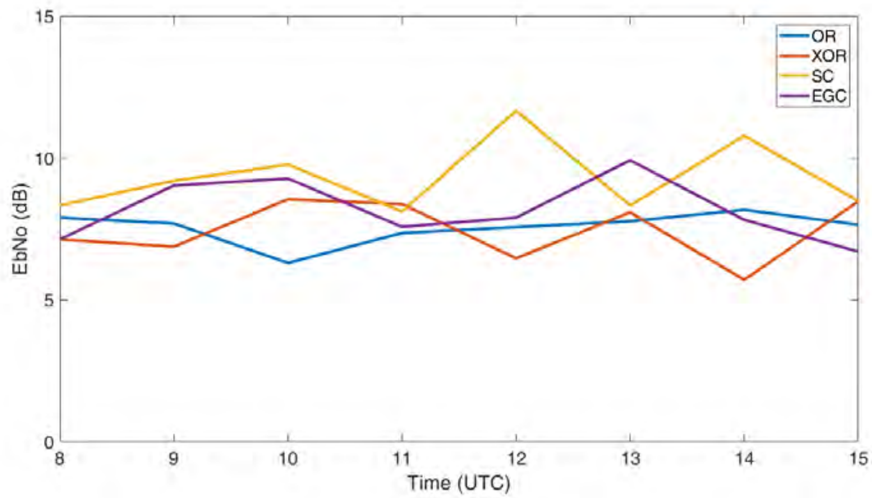

Figure 7. E_b/N_0 vs Time for 4QAM at 50 W.

Figure 7. E_b/N_0 vs Time for 4QAM at 50 W.

5.3. BER CDF According to Polarization Techniques

5.3. BER CDF According to Polarization Techniques

Once we have analyzed the main behavior characteristics of the signal received in different ways, we can analyze the behavior of different orders and modulations received by ionospheric waves or polarization techniques. First of all, we analyze the modulations of order 4. In Figure 8, we can see that the ordinary and extraordinary waves are affected in the same way as the 4PSK and 4QAM with a 80% probability to receive a BER lower than 10^{-4}. In contrast, the 4FSK has a 57% probability to receive a BER lower than 10^{-4}. On the other hand, the selection combining looks to be the best option for the three modulations. To achieve a BER lower than 10^{-4}, the 4PSK has a 96% probability, the 4FSK has a 88% probability, and the 4QAM has a 85% probability. In the case of using equal-gain combining to achieve a BER lower than 10^{-4}, the 4PSK and 4QAM has a 82% probability and the 4FSK has a 59% probability. For the BER CDF figures, we set a threshold at 10^{-4} because probabilistically we cannot ensure a BER lower than 10^{-4} due to the number of bits transmitted in all the test performed.

Once we have analyzed the main behavior characteristics of the signal received in different ways, we can analyze the behavior of different orders and modulations received by ionospheric waves or polarization techniques. First of all, we analyze the modulations of order 4. In Figure 8, we can see that the ordinary and extraordinary waves are affected in the same way as the 4PSK and 4QAM with a 80% probability to receive a BER lower than 10^{-4}. In contrast, the 4FSK has a 57% probability to receive a BER lower than 10^{-4}. On the other hand, the selection combining looks to be the best option for the three modulations. To achieve a BER lower than 10^{-4}, the 4PSK has a 96% probability, the 4FSK has a 88% probability, and the 4QAM has a 85% probability. In the case of using equal-gain combining to achieve a BER lower than 10^{-4}, the 4PSK and 4QAM has a 82% probability and the 4FSK has a 59% probability. For the BER CDF figures, we set a threshold at 10^{-4} because probabilistically we cannot ensure a BER lower than 10^{-4} due to the number of bits transmitted in all the test performed.

If we analyze the modulations of order 8, we can note a decrease of the probabilities to achieve lower BERs because of the decrease of the E_b/N_0 received. In Figure 9, we can see that to achieve a BER lower than 10^{-4} by the ionospheric waves, for the 8PSK we have between a 42% and 55% probability, for the 8FSK between a 8% and 26% probability, and the 8QAM between a 1% and 24% probability. In this case, selection combining is still the best option for the 8PSK and 8FSK with a 70% and 40% probability, respectively, to achieve a BER lower than 10^{-4}. For the 8QAM, selection combining and

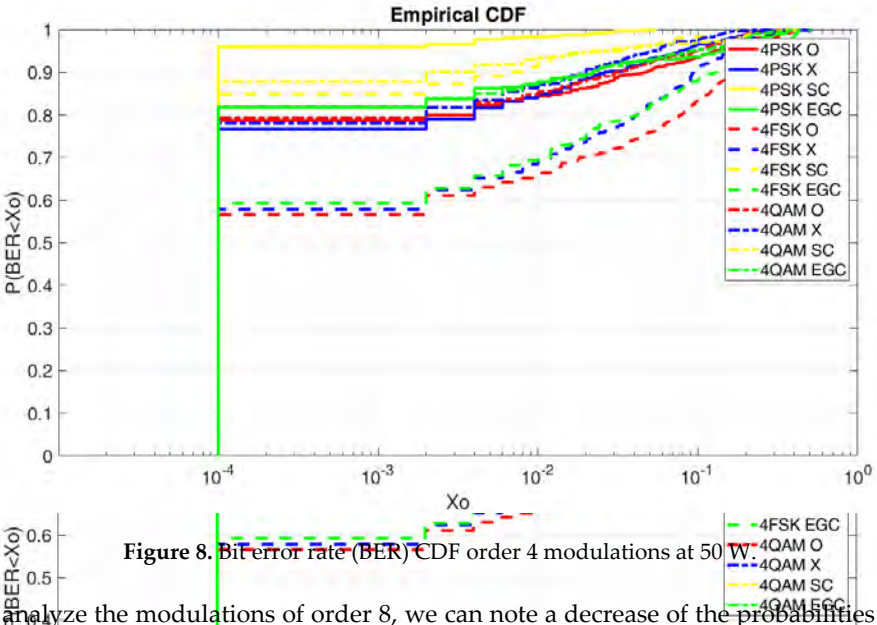

Figure 8. Bit error rate (BER) CDF order 4 modulations at 50 W.

If we analyze the modulations of order 8, we can note a decrease of the probabilities to achieve lower BERs because of the decrease of the E_b/N_0 received. In Figure 9, we can see that to achieve a BER lower than 10^{-4} by the ionospheric waves, for the 8PSK we have between a 42% and 55% probability, for the 8FSK between a 8% and 26% probability, and the 8QAM between a 1% and 24% probability. In this case, selection combining is still the best option for the 8PSK and 8FSK with a 70% and 40% probability, respectively, to achieve a BER lower than 10^{-4}. For the 8QAM, selection combining and equal-gain combining have the same results in this test, with a 39% probability to achieve a BER lower than 10^{-4}, which is the same for the equal-gain combining of 8FSK. The 8PSK by equal-gain combining has a 30% probability to achieve a BER lower than 10^{-4}.

Figure 8. Bit error rate (BER) CDF order 4 modulations at 50 W.

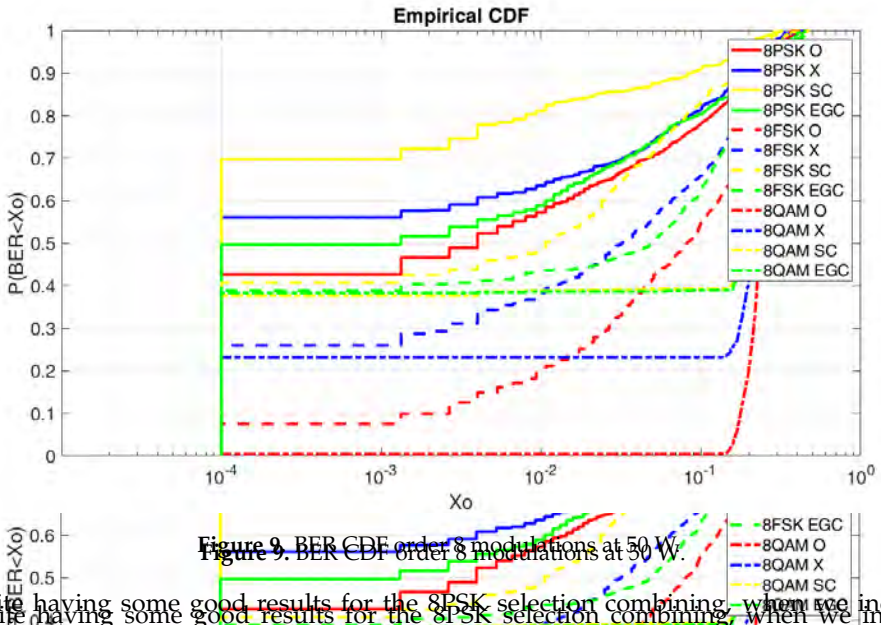

Figure 9. BER CDF order 8 modulations at 50 W.

Figure 9. BER CDF order 8 modulations at 50 W.

Despite having some good results for the 8PSK selection combining, when we increase the modulation order to 16, the power transmission is not enough to achieve an E_b/N_0 that is enough to obtain a lower E_b/N_0. As we can see in Figure 10, for 16QAM and 16FSK, to achieve a BER lower than 10^{-2} by the ionospheric waves, the probability is 1%. The 16PSK is the best option in this case in order to obtain about a 7% probability. The selection combining for the 16PSK brings the best result of the graphic with a 25% probability to receive a BER lower than 10^{-4} and for equal-gain combining a 21% probability to achieve the same result. Furthermore, 16QAM and 16FSK obtain a great improvement by the use of selection combining and equal-gain combining with the same results for both polarization techniques, nearly a 20% probability to obtain a BER lower than 10^{-4}.

Despite having some good results for the 8PSK selection combining, when we increase the modulation order to 16, the power transmission is not enough to achieve an E_b/N_0 that is enough to obtain a lower E_b/N_0. As we can see in Figure 10, for 16QAM and 16FSK, to achieve a BER lower than 10^{-2} by the ionospheric waves, the probability is 1%. The 16PSK is the best option in this case in order to obtain about a 7% probability. The selection combining for the 16PSK brings the best result of the graphic with a 25% probability to receive a BER lower than 10^{-4} and for equal-gain combining a 21% probability to achieve the same result. Furthermore, 16QAM and 16FSK obtain a great improvement by the use of selection combining and equal-gain combining with the same results for both polarization techniques, nearly a 20% probability to obtain a BER lower than 10^{-4}.

Figure 9. BER CDF order 8 modulations at 50 W.

Despite having some good results for the 8PSK selection combining, when we increase the modulation order to 16, the power transmission is not enough to achieve an E_b/N_0 that is enough to obtain a lower E_b/N_0. As we can see in Figure 10, for 16QAM and 16FSK, to achieve a BER lower than 10^{-2} by the ionospheric waves, the probability is 1%. The 16PSK is the best option in this case in order to obtain about a 7% probability. The selection combining for the 16PSK brings the best result of the graphic with a 25% probability to receive a BER lower than 10^{-4} and for equal-gain combining a 21% probability to achieve the same result. Furthermore, 16QAM and 16FSK obtain a great improvement by the use of selection combining and equal-gain combining with the same results for both polarization techniques, nearly a 20% probability to obtain a BER lower than 10^{-4}.

Appl. Sci. **2020**, *10*, x FOR PEER REVIEW 12 of 16

by the use of selection combining and equal-gain combining with the same results for both polarization techniques, nearly a 20% probability to obtain a BER lower than 10^{-4}.

by the use of selection combining and equal-gain combining with the same results for both polarization techniques, nearly a 20% probability to obtain a BER lower than 10^{-4}.

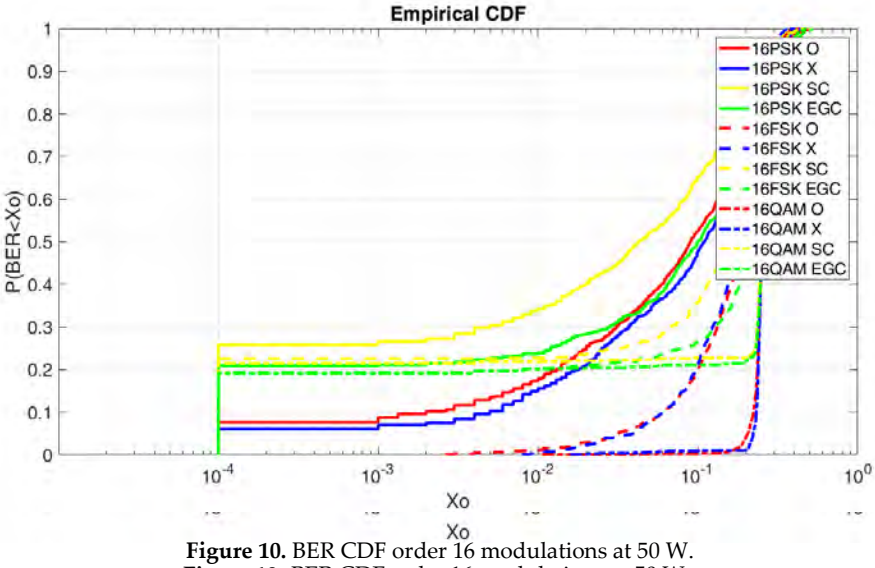

Figure 10. BER CDF order 16 modulations at 50 W.

Figure 10. BER CDF order 16 modulations at 50 W.

5.4. BER CDF According to Power Transmission

5.4. BER CDF According to Power Transmission
5.4. BER CDF According to Power Transmission

As we have seen, the power transmission of 50 W is not enough to obtain good results for higher modulation orders. The modulations of order 16 denotes a high decrease of the probabilities to achieve low BERs. Despite the results, we have seen that selection combining brings us the best results, especially for PSK modulation. However, a power transmission of 50 W is high, so taking into account these conclusions, we analyze the behavior of the PSK modulation orders 4 and 8 for a power transmission between 6 W and 50 W. As we can see in Figure 11, the modulation 4PSK brings the best results in comparison to the 8PSK, regardless the power transmission. Even so, the bitrate of the 8PSK is higher. As the graphic shows, 4PSK with a power transmission of 50 W, 25 W, 12 W, and 6 W have probabilities of 96%, 94%, 92%, and 71%, respectively, to achieve a BER lower than 10^{-4}. The 8PSK with a power transmission of 50 W, 25 W, and 12 W have probabilities of 69%, 50%, 32%, and 30%, respectively, to achieve a BER lower than 10^{-4}.

As we have seen, the power transmission of 50 W is not enough to obtain good results for higher modulation orders. The modulations of order 16 denotes a high decrease of the probabilities to achieve low BERs. Despite the results, we have seen that selection combining brings us the best results, especially for PSK modulation. However, a power transmission of 50 W is high, so taking into account these conclusions, we analyze the behavior of the PSK modulation orders 4 and 8 for a power transmission between 6 W and 50 W. As we can see in Figure 11, the modulation 4PSK brings the best results in comparison to the 8PSK, regardless the power transmission. Even so, the bitrate of the 8PSK is higher. As the graphic shows, 4PSK with a power transmission of 50 W, 25 W, 12 W, and 6 W have probabilities of 96%, 94%, 92%, and 71%, respectively, to achieve a BER lower than 10^{-4}. The 8PSK with a power transmission of 50 W, 25 W, and 12 W have probabilities of 69%, 50%, 32%, and 30%, respectively, to achieve a BER lower than 10^{-4}.

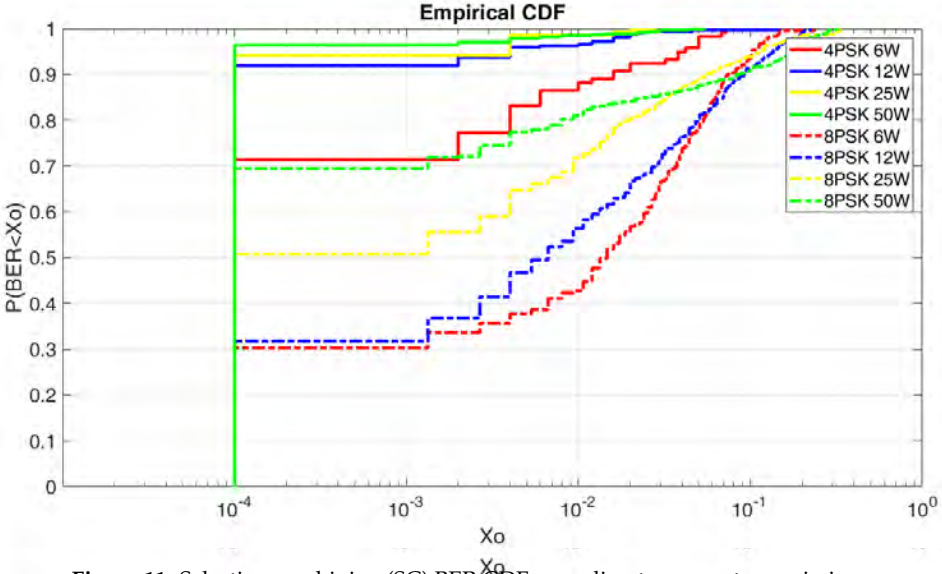

Figure 11. Selection combining (SC) BER CDF according to power transmission.

Figure 11. Selection combining (SC) BER CDF according to power transmission.

5.5. Number of Transmissions According to Selection Combining

To form conclusions about which could be the best order modulation and power transmission to use with selection combining, we analyze, based on a Bernoulli distribution, the probability to receive a BER lower than 10^{-4} after several retransmissions. Analyzing the results in Figure 12. Number of transmissions according to selection combining, we can see that making use of a 4PSK with a power transmission of 12 W, 25 W, and 50 W, we have probabilities of 99% to achieve a BER lower than 10^{-4} if we retransmit the packet. In the case of using a 4PSK with a power transmission of 6 W or an 8PSK with a power transmission of 50 W, we have nearly the same results. To achieve a 99% probability to obtain a BER lower than 10^{-4}, it would be necessary to have 4 transmissions. With two transmissions, we can obtain probabilities of 91% to achieve a BER lower than 10^{-4}, and with three transmissions, probabilities of 97% can be obtained to achieve a BER lower than 10^{-4}.

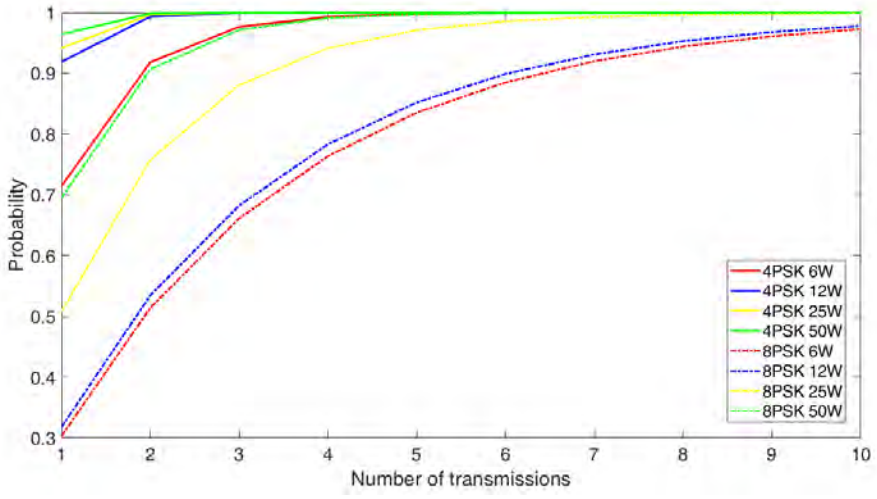

Figure 12. Number of transmissions according to selection combining.

6. Conclusions

After analyzing the results obtained, we observed that the ordinary and extraordinary waves are not received with the same E_b/N_0, which as we have seen can differ up to 3 dB. These E_b/N_0 differences can provide us the possibility to apply polarization diversity techniques to take advantage of this fact.

First of all, we can conclude that selection combining helps us receive the highest E_b/N_0 between ordinary and extraordinary waves. Consequently, by this polarization technique, we can receive meanly lower BER results. On the other hand, equal-gain combining is also a polarization technique that can obtain an E_b/N_0 3 dB higher than the highest E_b/N_0 received by the ordinary and extraordinary waves. However, this possibility depends on the received electromagnetic noise, and it is limited to a 1% probability, but it is 20% probable to receive a higher E_b/N_0 than the highest received by the ordinary and extraordinary waves.

Taking these results into account, if we make use of PSK, FSK, and QAM modulations orders between 2 and 32 with a power transmission of 50 W, we analyzed that even with using polarization techniques, the BER obtained for modulations of order up to 16 is not low enough to ensure communication. Moreover, analyzing the results, we see that by PSK modulations with selection combining, we obtain the best BER results. For 4PSK and 8PSK modulations with selection combining and power transmissions variations between 6 and 50 W, we can observe that the best BER results are similar for 4PSK with power transmissions between 12 and 50 W. The second best BER results obtained are for 4PSK with 6 W and 8PSK with 50 W.

In conclusion, we summarized in Table 2 three different options depending on the application and needs of the remote sensing system.

Table 2. Application summary.

Power Consumption	Polarization Technique	Modulation	Bitrate	Probability to BER 10^{-4}
6 W	SC	4PSK	2.9 Kbps	71%
12 W	SC	4PSK	2.9 Kbps	92%
50 W	SC	8PSK	5.8 Kbps	70%

If our remote sensing system requires a low power usage, we can opt to use of a 4PSK with a power transmission of 6 W. In this case, we have a 71% probability to receive a BER lower than 10^{-4} and a 99% probability if we make two retransmissions in the worst case. If our remote sensing system can make use of high power transmissions, the best option will be the usage of the 8PSK with 50 W. This case will offer double the bitrate than 4PSK as well as a probability of 70% to receive a BER lower than 10^{-4} and a probability of 99% if we make two retransmissions in the worst case. Lastly, if our remote sensing system requires low power consumption and needs to receive all packets with a minimum of retransmissions, we can choose a 4PSK with a power transmission of 12 W. In this case, we have a 92% probability to receive a BER lower than 10^{-4} and a 99% probability if we make one retransmission. Moreover, the application of an error correction code (ECC) will highly increase the probabilities of receiving correctly the first packet transmitted. On the other hand, polarization techniques can compensate for the lower gains of compact antennas, making more feasible the use of them on HF communications. In addition, remote systems allow for using low power transmissions, which will decrease battery consumption and will make more feasible the use of renewable energies.

Author Contributions: Investigation, J.M.M., J.M. and J.P.; Methodology, J.L.P. and D.B.; Software, J.M.M., J.M. and J.P.; Supervision, J.L.P. and D.B.; Validation, J.L.P. and D.B.; Writing—original draft, J.M.M., J.M. and J.P.; Writing—review & editing, J.M.M., J.M., J.P., J.L.P. and D.B. All authors have read and agreed to the published version of the manuscript.

Funding: This research was funded by the Spanish Ministry on Science, Innovation and University, the Investigation State Agency and the European Regional Development Fund (ERDF) under the grant number RTI2018-097066-B-I00 (MCIU/AEI/FEDER, UE) for the project "NVIS SENSOR NETWORK FOR THE SOUTH SHETLAND ISLANDS ARCHIPELAGO" (SHETLAND-NET).

Conflicts of Interest: The authors declare no conflict of interest.

References

1. Lauridsen, M.; Nguyen, H.; Vejlgaard, B.; Kovacs, I.Z.; Mogensen, P.; Sorensen, M. Coverage Comparison of GPRS, NB-IoT, LoRa, and SigFox in a 7800 km^2 Area. In Proceedings of the 2017 IEEE 85th Vehicular Technology Conference (VTC Spring), Sydney, Australia, 4–7 June 2017; pp. 1–5.
2. Bechthum, E.; El Soussi, M.; Dijkhuis, J.; Mateman, P.; van Schaik, G.J.; Breeschoten, A.; Liu, Y.H.; Bachmann, C.; Philips, K. A CMOS polar single-supply class-G SCPA for LTE NB-IoT and cat-M1. In Proceedings of the ESSCIRC 2018-IEEE 44th European Solid State Circuits Conference (ESSCIRC), Dresden, Germany, 3–6 September 2018; pp. 30–33.
3. Porte, J.; Maso, J.M.; Pijoan, J.L.; Badia, D. Sensing system for remote areas in Antarctica. *Radio Sci.* **2020**. [CrossRef]
4. Porte, J.; Maso, J.; Pijoan, J.L.; Miret, M.; Badia, D.; Jayasinghe, J. Education and e-health for developing countries using NVIS communications. In Proceedings of the 2018 IEEE Region 10 Humanitarian Technology Conference (R10-HTC), Malambe, Sri Lanka, 6–8 December 2018; pp. 1–5.
5. Porte, J.; Maso, J.M.; Pijoan, J.L.; Badia, D. Design, implementation, and test of an SDR for NVIS communications. *Int. J. Circuit Theory Appl.* **2019**, *47*, 1502–1512. [CrossRef]
6. Maso, J.; Porte, J.; Pijoan, J.L.; Badia, D. Internet of things communications for remote sensors in Antarctica using NVIS. *HF Nordic*. 2019. Available online: https://www.researchgate.net/profile/Joaquim_Porte_Jimenez/publication/335774336_INTERNET_OF_THINGS_COMMUNICATIONS_FOR_REMOTE_SENSORS_IN_ANTARCTICA_USING_NVIS/links/5d7a60354585157fde0fce47/INTERNET-OF-THINGS-COMMUNICATIONS-FOR-REMOTE-SENSORS-IN-ANTARCTICA-USING-NVIS.pdf (accessed on 26 May 2020).

7. Porte, J.; Pijoan, J.L.; Masó, J.M.; Badia, D.; Zaballos, A.; Alsina-Pagès, R.M. Advanced HF communications for remote sensors in Antarctica. In *Antartica—A Key to Global Change*, 1st ed.; IntechOpen: London, UK, 2019; Available online: https://www.intechopen.com/books/antarctica-a-key-to-global-change/advanced-hf-communications-for-remote-sensors-in-antarctica (accessed on 27 May 2020).
8. Orga, F.; Hervas, M.; Alsina-Pages, R.M. Flexible Low-Cost SDR Platform for HF Communications: Near vertical incidence skywave preliminary results. *IEEE Antennas Propag. Mag.* **2016**, *58*, 49–56. [CrossRef]
9. Wilson, J.M. *A Low Power HF Communication System*; Univesity of Manchester: Manchester, UK, 2012.
10. Davies, K. *Ionospheric Radio*; The Institution of Engineering and Technology (IET): Stevenage, UK, 1990.
11. Hervás, M.; Pijoan, J.L.; Alsina-Pagès, R.M.; Salvador, M.; Altadill, D. Channel Sounding and Polarization Diversity for the NVIS Channel. 2013. Available online: https://www.researchgate.net/profile/Marcos_Hervas/publication/256375415_CHANNEL_SOUNDING_AND_POLARIZATION_DIVERSITY_FOR_THE_NVIS_CHANNEL/links/0deec522664e6509e4000000/CHANNEL-SOUNDING-AND-POLARIZATION-DIVERSITY-FOR-THE-NVIS-CHANNEL.pdf (accessed on 26 May 2020).
12. Witvliet, B.A.; Alsina-Pagès, R.M. Radio communication via Near Vertical Incidence Skywave propagation: An overview. *Telecommun. Syst.* **2017**, *66*, 295–309. [CrossRef]
13. Erhel, Y.; Lemur, D.; Oger, M.; Le Masson, J.; Marie, F. Evaluation of Ionospheric HF MIMO Channels: Two complementary circular polarizations reduce correlation. *IEEE Antennas Propag. Mag.* **2016**, *58*, 38–48. [CrossRef]
14. Li, P.; Liang, C.H.; Tian, J. Polarization diversity experiments in HF communication. In Proceedings of the ISAPE 2003—2003 6th International Symposium on Antennas, Propagation and EM Theory, Proceedings, Beijing, China, 28 October–1 November 2003; pp. 556–559.
15. Witvliet, B.A.; Van Maanen, E.; Petersen, G.J.; Westenberg, A.J.; Bentum, M.J.; Slump, C.H.; Schiphorst, R. The importance of circular polarization for diversity reception and MIMO in NVIS propagation. In Proceedings of the 8th European Conference on Antennas and Propagation (EuCAP 2014), The Hague, The Netherlands, 6–11 April 2014; pp. 2797–2801.
16. Umaisaroh, U.; Hendrantoro, G.; Mauludiyanto, A.; Fukusako, T. Capacity of 2×2 MIMO HF NVIS Channels With Linearly Polarized Horizontal Antennas. *IEEE Wirel. Commun. Lett.* **2019**, *8*, 1120–1123. [CrossRef]
17. Greenman, M. An Introduction to HF propagation and the Ionosphere. *QSL*. Available online: https://www.qsl.net/zl1bpu/IONO/iono101.htm (accessed on 27 May 2020).
18. Witvliet, B.A. *Near Vertical Incidence Skywave: Interaction of Antenna and Propagation Mechanism*; Universiteit Twente: Enschede, The Netherlands, 2015.
19. Valenzuela-valdes, J.F.; Garcia-fernandez, M.A.; Martinez-gonzalez, A.M.; Sanchez-Hernandez, D. The Role of Polarization Diversity for MIMO Systems Under Rayleigh-Fading Environments. *IEEE Antennas Wirel. Propag. Lett.* **2006**, *5*, 534–536. [CrossRef]
20. Red Pitaya. Available online: https://www.redpitaya.com/ (accessed on 4 June 2019).
21. Xilinx and Inc. Zynq-7000 SoC First Generation Architecture. Available online: https://www.xilinx.com/support/documentation/data_sheets/ds190-Zynq-7000-Overview.pdf (accessed on 27 May 2020).
22. Xilinx Zynq-7000 SoC ZC702 Evaluation Kit. Available online: https://www.xilinx.com/products/boards-and-kits/ek-z7-zc702-g.html (accessed on 20 January 2020).
23. Thomas, S.A.; Anusudha, K. Comparative analysis for various parametric attributes for an optimized DUC/DDC. In Proceedings of the 2017 International Conference on Inventive Computing and Informatics, ICICI 2017, Hotel Arcadia, Coimbatore, India, 23–24 November 2017; pp. 206–209.
24. Austin, R.; Bull, P.; Buffery, S. A raspberry Pi based scalable software defined network infrastructure for disaster relief communication. In Proceedings of the 2017 IEEE 5th International Conference on Future Internet of Things and Cloud, FiCloud 2017, Prague, Czech Republic, 21–23 August 2017; Volume 2017, pp. 265–271.
25. Elektronik, B. Bonn Elektronik Power amplifier 9 kHz–40 Ghz. Available online: https://allice.de/wp-content/uploads/2017/03/Bonn-Katalog-Web.pdf (accessed on 27 May 2020).
26. R2015a—MATLAB & Simulink—MathWorks España. Available online: https://es.mathworks.com/help/matlab/release-notes-R2015a.html (accessed on 29 September 2019).

27. Observatori de l'Ebre. Available online: http://www.obsebre.es/es/ (accessed on 21 February 2020).
28. Proakis, J.G. *Digital Communications*; McGraw-Hill: University of California, San Diego, CA, USA, 1995.

Bibliography

[1] M. Lauridsen et al. "Coverage Comparison of GPRS, NB-IoT, LoRa, and SigFox in a 7800 km^2 Area". In: *2017 IEEE 85th Vehicular Technology Conference (VTC Spring)*. 2017, pp. 1–5.

[2] E. Bechthum et al. "A CMOS Polar Single-Supply Class-G SCPA for LTE NB-IoT and Cat-M1". In: *ESSCIRC 2018 - IEEE 44th European Solid State Circuits Conference (ESSCIRC)*. 2018, pp. 30–33.

[3] Maso J.M. et al. "Ionospheric Polarization Techniques for Robust NVIS Remote Sensing Platforms". In: *Appl. Sci.* (2020). DOI: 10.3390/app10113730.

[4] Ben A. Witvliet. "Near Vertical Incidence Skywave: Interaction of antenna and propagation mechanism". English. PhD thesis. University of Twente, Dec. 2015. ISBN: 978-90-365-3938-8. DOI: 10.3990/1.9789036539388.

[5] Ismael Pellejero Ibáñez. "COMUNICACIONES NVIS EN HF". In: *Revista de la Unión de Radioaficionados Españoles (URE)* (2008).

[6] Wikipedia. *The ionosphere*. URL: https://en.wikipedia.org/wiki/Ionosphere.

[7] Jordi Malé Carbonell. *Study of Polarization Diversity and SIMO Systems for NVIS Technologies*. Tech. rep. La Salle in Ramon Llull University, Barcelona, Spain, 2019.

[8] Ben A. Witvliet and Rosa Ma Alsina-Pagès. "Radio communication via Near Vertical Incidence Skywave propagation: an overview". In: *Telecommunication Systems* 66.2 (Oct. 2017), pp. 295–309. ISSN: 1572-9451. DOI: 10.1007/s11235-017-0287-2. URL: https://doi.org/10.1007/s11235-017-0287-2.

[9] QSL. *The Ionosphere - an Introduction*. URL: https://www.qsl.net/zl1bpu/IONO/iono101.htm.

[10] Joan Claudi Socoró Rosa Ma Alsina. *Comunicacions en entorns hostils*. Tech. rep. La Salle in Ramon Llull University, Barcelona, Spain, 2018.

[11] Marta Miret Badia. *Digital Emergency Communications for the isolated High-Andean communities in Valle Sagrado*. Tech. rep. La Salle in Ramon Llull University, Barcelona, Spain, 2018.

[12] Joaquim Porte Jiménez. *Estudi Canal Comunicació NVIS Barcelona - Cambrils*. Tech. rep. La Salle in Ramon Llull University, Barcelona, Spain, 2016.

[13] R. U. Nabar et al. "Performance of multiantenna signaling techniques in the presence of polarization diversity". In: *IEEE Transactions on Signal Processing* 50.10 (Oct. 2002), pp. 2553–2562. ISSN: 1053-587X. DOI: 10.1109/TSP.2002.803322.

[14] J. F. Valenzuela-valdes et al. "The Role of Polarization Diversity for MIMO Systems Under Rayleigh-Fading Environments". In: *IEEE Antennas and Wireless Propagation Letters* 5 (2006), pp. 534–536. ISSN: 1536-1225. DOI: 10.1109/LAWP.2006.889552.

[15] T. Eng, Ning Kong, and L. B. Milstein. "Comparison of diversity combining techniques for Rayleigh-fading channels". In: *IEEE Transactions on Communications* 44.9 (Sept. 1996), pp. 1117–1129. ISSN: 0090-6778. DOI: 10.1109/26.536918.

[16] Wikipedia. *Diversity Combining*. URL: https://en.wikipedia.org/wiki/Diversity_combining.

[17] Wikipedia. *Diversity Gain*. URL: https://en.wikipedia.org/wiki/Diversity_gain.

[18] S.Loyka. *Diversity Combining Techniques*. Tech. rep. La Salle in Ramon Llull University, Barcelona, Spain, 2015.

[19] Dragan Mitić et al. "An overview and analysis of BER for three diversity techniques in wireless communication systems". In: *Yugoslav Journal of Operations Research* 25 (Jan. 2014), pp. 7–7. DOI: 10.2298/YJOR131120007M.

[20] Josep M. Masó Llinàs. *Estudio de modulaciones digitales de baja potencia y anchos de banda variable en la Antártida*. Tech. rep. La Salle in Ramon Llull University, Barcelona, Spain, 2019.

[21] Joaquim Porte et al. "Sensing System for Remote Areas in Antarctica". In: *Radio Science* 55.3 (2020). e2019RS006920 2019RS006920, e2019RS006920. DOI: 10.1029/2019RS006920. eprint: https://agupubs.onlinelibrary.wiley.com/doi/pdf/10.1029/2019RS006920. URL: https://agupubs.onlinelibrary.wiley.com/doi/abs/10.1029/2019RS006920.

[22] Mathworks. *QPSK Contellation*. URL: https://es.mathworks.com/help/comm/ref/comm.qpskdemodulator.constellation.html.

[23] StemLab. *The RedPitaya*. URL: https://www.redpitaya.com.

[24] Xilinx. *Xilinx and Inc. Zynq-7000 SoC First Generation Architecture*. URL: https://www.xilinx.com/support/documentation/data_sheets/ds190-Zynq-7000-Overview.pdf.

[25] Xilinx. *Xilinx Zynq-7000 SoC ZC702 Evaluation Kit*. URL: https://www.xilinx.com/products/boards-and-kits/ek-z7-zc702-g.html.

[26] Sherin Thomas and K. Anusudha. "Comparative analysis for various parametric attributes for an optimized DUC/DDC". In: Nov. 2017, pp. 206–209. DOI: 10.1109/ICICI.2017.8365339.

[27] RaspberryPi. *RaspberryPi 3 Model B*. URL: https://www.raspberrypi.org/products/raspberry-pi-3-model-b/.

[28] Observatori de l'Ebre. *Ebre Ionograms*. 2019. URL: http://www.obsebre.url.edu/ca/ionogrames-revisats.

[29] Pau Bergada et al. "Remote Sensing and Skywave Digital Communication from Antarctica". In: *Sensors (Basel, Switzerland)* 9 (Dec. 2009), pp. 10136–57. DOI: 10.3390/s91210136.

[30] Mathworks. *R2015a - MATLAB Simulink - Mathworks España*. URL: https://es.mathworks.com/help/matlab/release-notes-R2015a.html.

[31] J. G. Proakis. *Digital communications*. McGraw-Hill, 1995.

[32] Marcos Hervas et al. "CHANNEL SOUNDING AND POLARIZATION DIVERSITY FOR THE NVIS CHANNEL". In: Aug. 2013.

[33] Wikipedia. *Outlier*. URL: https://en.wikipedia.org/wiki/Outlier.

[34] 5G Technology World. *The basics of 5G's modulation, OFDM*. URL: https://www.5gtechnologyworld.com/the-basics-of-5gs-modulation-ofdm/.